Columbia University
New York, N.Y. 10027

NASA Cooperative Agreement NCC 5-29

Semi-Annual Progress Report

April 1992 - September 1992

A STRATEGY FOR ESTIMATING THE IMPACT OF CO_2 FERTILIZATION ON SOIL CARBON STORAGE

Kevin Harrison and Wallace Broecker

7/16/92

Department of Geochemistry, Lamont-Doherty Geological Observatory, Columbia University, Palisades, New York

to be submitted for Global Biogeochemical Cycles, July 1992

ABSTRACT:

As soils are the most likely candidate for the so-called missing carbon sink, we explore the possible impact of CO_2 fertilization on the global humus inventory. For any given greening-induced enhancement of plant growth, the increase in soil carbon inventory will depend on the spectrum of turnover times with respect to oxidation. Here, we develop estimates of carbon turnover rates from soil radiocarbon measurements.

INTRODUCTION:

The so-called missing carbon sink is the difference between the amount of carbon released by fossil fuel burning and deforestation, and the amount of excess carbon which has appeared in the atmosphere and ocean reservoirs (figure 1 and table 1). When combined with the atmospheric increase, most estimates of oceanic CO_2 uptake (Keeling, 1973; Oeschger et al., 1975; Broecker et al., 1979; Bacastow and Bjorkstrom, 1981; Peng, 1986; Maier-Reimer and Hasselmann, 1987; Keeling et al., 1989a,b and Toggweiler et al., 1989a,b) fall short of matching fossil fuel CO_2 released during the same time interval. Thus, the missing sink is generally thought to

be at least as large as deforestation (table 1). If Houghton's (1990) estimates of biospheric release are used (figure 1 and table 1), over the period 1958 to 1978, about 37 GtC (or 1.8 GtC/year, Sarmiento and Sundquist, 1992) are unaccounted for. This bookkeeping does not include processes such as CO_2 fertilization and N deposition, which could stimulate terrestrial carbon storage.

One promising prospect for the missing sink is greening of the terrestrial biosphere through CO_2 fertilization of plant growth. Today's atmosphere contains 25% more CO_2 than did the atmosphere in 1800 (Neftal et al., 1985 and Bacastow and Keeling, 1981). The average growth enhancement factor (i.e. percent increase in plant growth rate divided by percent increase in atmospheric CO_2 content) found in short term chamber experiments is 0.35 (Esser, 1987, Kohlmaier et al., 1989 and Bazzaz et al, 1992). If these experiments are applicable to the natural environment, then between 1850 and today, the rate of plant growth should have increased by 9%. But the use of limited, short-term chamber experiments to estimate real-world response is highly controversial. For example, the experiments neglect the natural limitations imposed by nitrogen availability. Indeed, the long-term experimental results of Norby et al. (1992) demonstrate no significant increase in plant biomass for yellow-poplar trees grown for years in enriched CO_2 environments; however, these authors do report increased root turnover and increased carbon dioxide flux out of the soil. Perhaps, soil carbon increased. At least for some regions, N is no longer limiting because of anthropogenic deposition of NH_3 and NO_3 (Kauppi et al., 1992). Duce et al. (1991) estimate that 0.05 Gt of oxidized N and 0.054 Gt of reduced N are deposited on land and in the oceans annually. Even if a relatively low carbon/nitrogen ratio of 10 is adopted, utilization of this nitrogen by the global ecosystem would sequester 1 GtC per year.

MODELING APPROACH:

Parton et al. (1987 and 1988) have developed the Century model and Jenkinson (1990) has developed the Rothemsted model for studying soil organic matter inventories. The structure of the two models is similar. For example, both estimate the flux of plant residue into three soil compartments: active, slow and passive.

The Century model calculates the climate change response of soil organic matter inventories for a grassland ecosystem. It's not clear that these results can be applied to other ecosystems. The parameters showing the greatest sensitivity are the turnover times for the slow and passive soil pools. These terms have been estimated indirectly for long-term incubation experiments.

The Rothamsted model's structure is similar to the Century model and is equally sensitive to the turnover time estimates for the slow and passive soil pools. Jenkinson estimates his turnover times by using data from carbon inventory changes in long-term agricultural experiments.

Here, we present a strategy for estimating turnover times more directly using radiocarbon measurements. To explore the dynamics of CO_2 fertilization's influence on soil carbon storage, we have developed a simple model. We assume that the carbon inventory for the world's soils was at steady state in the year 1850 (i.e., the input flux via litter and roots equaled the output flux via bacterial decomposition). We perturb the system by increasing the level of atmospheric CO_2 (following observed time history from 1850 to the present) and assume a CO_2 fertilization factor of 0.35 for the carbon flux into the soil box. This, in turn, causes the inventory of soil carbon to rise. However, as the carbon inventory increases, so does the rate of soil respiration (we assume that a fixed fraction of the soil organic carbon is oxidized to

CO_2 in each year's time step). We further assume that the change in global temperature over this interval has been too small to increase rates. Soil carbon accumulates because the rise in the rate of decomposition lags the rise in the rate of input. This lag depends on the spectrum of residence times of carbon atoms in the soil.

Clearly, no single residence time can characterize the complex of organic compounds in soils. Nor can the most appropriate residence time for any one soil be applied to others. Even the determination of the portion of the soil carbon falling into broad residence time bands currently lies beyond our grasp. As outlined below, we simplify the problem by dividing soil organics into that portion which has a mean residence time too long to significantly respond to a perturbation with an e- folding time of 30 years (the mean age of fossil fuel CO_2 molecules), and into that portion with residence times short enough to show a significant response. We use radiocarbon data to assign a single average residence time to each of these reservoirs.

Perturbations, like CO_2 fertilization, have the greatest impact on carbon pools having short residence times, and the least influence on carbon pools having long residence times. For example, the carbon pool having a residence time of a few years increases its carbon inventory by 9% (figure 2). In contrast, pools with residence times greater than 1000 years experience almost no change. A carbon pool having a 25-year residence time will show an increase of 5.3%.

Tracer experiments provide a way to estimate soil-carbon residence times. Two global carbon tracer experiments include diluting and enhancing the C-14 content of the atmosphere. We define R as the measured C-14/C ratio of the sample divided by the C-14/C ratio of 1850 wood. R(atmosphere) decreased by 2.5% between 1850 and 1950 as the result of burning fossil fuel. This dilution's impact would be difficult to detect. However, nuclear bombs increased R(soil) from 1950 to 1963, to almost 1.9. In 1963, nuclear tests were banned and since then R(atmosphere) has decreased

exponentially. This near-doubling of R(atmosphere) should be reflected in the fast-cycling pools in soil (figure 3). The three-year pool follows the atmospheric signal, although its maximum occurs later and has a smaller amplitude. Longer residence-time pools have ever smaller maxima occurring at ever later times.

EXPERIMENTAL RESULTS:

We have obtained radiocarbon data for native sites from four locations: Lodi, Italy; Duke Experimental Forest near Durham, North Carolina; the Konza Prairie in Manhattan, Kansas; and two sites near Saskatoon, Saskatchewan, Canada (see table 2 and Schoenau, 1988). Our sample treatment included hand picking of visible plant and root debris and floating in water of charcoal and smaller plant debris. Carbonates have been removed with dilute acid. The remaining organic carbon has been oxidized to carbon dioxide and subsequently reduced to form graphite targets for accelerator mass spectrometry.

In addition to our results, we summarize literature values. The locations of the sampling sites are plotted in figure 4. Although our literature search has been reasonably comprehensive, data are scant.

When the native soil radiocarbon values are plotted against time (figure 5), a trend becomes apparent. The limited number of pre-nuclear soils show values below atmospheric averaging 0.90 (table 2). The values rise during the 1960's and flatten thereafter at a value of 1.15.

INTERPRETING RADIOCARBON MEASUREMENTS USING MODEL RESULTS:

A one-component model fails to explain the observed R(soil) increase from pre-bomb to present-day values (figure 5). For example, the average pre-1963 R(soil) value (table 2) is 0.90 (850 years). Our model predicts that carbon having a turnover time of 850 years will show little bomb C-14 build-up, but R(soil)observations exceed 1.1. Hence, soil carbon pools must have a continuum of exchange rates ranging from very slow to relatively fast. We have modeled the soil carbon system with two components, one slow and one fast.

Our strategy is to find a combination of amount and residence time for both of these fractions so as to fit the mean of the observations. In our first attempt to do this, we have assigned a mean residence time of 3,700 years to the slow fraction and 25 years to the fast fraction. If we make the fast fraction 75% of the total and the slow fraction 25% of the total, we achieve a fair fit to both the pre-bomb average and the post-bomb data points (figure 7).

We arrive at this breakdown as follows: We assume that deep in the soil zone the fast-cycling component is gone. Hence, the R measured deep in the soils provides an estimate of the slow-cycling component's turnover time. The available deep soil radiocarbon values, listed in table 3, average 0.63, which corresponds to a 3,700-year residence time. For the fast-cycling pool, we find by iteration that a 25-year residence time pool gives the best fit. Specifically, we show how bomb radiocarbon would build up in soil carbon pools having 3,700-, 100-, 25- and 10-year residence times (figure 6). We add 25% of the slow pool to 75% of the fast pool to replicate the 0.90 pre-bomb R(soil) value. We superimpose the experimental observations over our

model prediction to find that a 25-year residence time for the fast pool provides the best fit to the data (figure 7).

A better fit could presumably be achieved by dividing the fast turnover reservoir into several sub-parts, each with its own residence time. We show one such example in figure 8. A combination of sub-parts, one with a 10-year and the other with a 100-year turnover time does not make a significant improvement. Our conclusion is that further subdivision of the fast reservoir is not warranted until a far larger data set is available.

While our approach is crude, it does advance and provide a template for future research. If a larger set of measurements on deep soil, pre-bomb soils and bomb-era soils were available, we could make estimates of soil residence times for specific ecosystems. In particular, measurements on soil samples collected in the early 1970's, when R(soil) values diverge for the differing residence times (figure 3) are needed.

USING CARBON RESIDENCE TIMES TO ASSESS THE IMPACT OF CO_2 FERTILIZATION:

Based on the fast-cycling pool's size and residence time, we can estimate the amount of additional carbon that has been sequestered because of CO_2 fertilization. To calculate the global inventory of fast-cycling carbon, we need to know the fraction of global soil containing rapid turnover carbon. Using soil radiocarbon and carbon content profiles, we estimate that 45% of the soil column contains fast-cycling carbon. Schlesinger (1991) estimates that 1500 GtC are sequestered globally in soil. We subtract 500 GtC from this global total to remove ecosystems with small amounts of fast-cycling carbon, such as boreal, tundra, alpine and swamp ecosystems (table 4). Hence, we estimate the global fast-cycling carbon pool to be 450 GtC (1000 GtC times 0.45, table 6). Using a 25-year residence time and applying a 0.35 greening

factor, this translates into a 24 GtC seqestration since 1850 (or 7 GtC from 1958 to 1978 or 0.6 GtC/year during the 1980's).

This approach ignores litter and fine root storage. In our study, these components have been physically removed from the soil. The litter pool size is about 55 GtC (Schlesinger, 1991) and has an average residence time of three years (Esser, 1987). A three-year residence time translates into a 7% carbon inventory increase (table 5). If we assume about the same input from fine root turnover, then 7 GtC from fine roots and litter have been sequestered because of CO_2 fertilization since 1850.

We have also failed to consider the increase in vegetation biomass. If we use a 1.5-year residence time for short-lived vegetation having a 90 GtC inventory and a 63-year residence time for a long-lived 500 GtC pool (Warneck, 1988), we estimate that the short-lived pool sequesters 0.2 and the long-lived pool sequesters 0.4 GtC annually (figure 9). If we combine the amount of carbon sequestered due to CO_2 fertilization in soil, litter, fine roots and vegetation, we calculate that about 57 GtC have been stored from 1850 to 1985, 17 GtC from 1958 to 1978, and 1.5 GtC annually for the 80's (table 5). Therefore, about 80% of the annual missing sink of 1.8 GtC/year (IPCC, 1990) might be explained by CO_2 fertilization.

CONCLUSION:

We have developed a model that estimates soil carbon residence times from soil radiocarbon measurements. We use these residence times to predict the extent of soil carbon's response to CO_2 fertilization. We hope this approach will serve as a strategy for future research.

ACKNOWLEDGEMENTS:

Jim Simpson and Inez Fung helped this project evolve with their insightful questions, patient discussions and modelling insights. Eric Haney and Peter Harrell helped select the Duke Experimental Forest field sites and did considerable work in constructing the two-meter deep soil pits. Bill Schlesinger, Dan Richter, and Norm Christenson hosted my visit to Duke, helped select field sites and shared their expertise in many discussions that helped me clarify my research objectives. Jeff Schoenau hosted my visit to the University of Saskatchewan, provided soil samples and supporting data, and made valuable suggestions for further research. Michel Ransom hosted my visit to Kansas State University, and in conjunction with Bill Wehmueller. helped me select field sites and use the soil probe truck. We thank Dr. Edoardo A. C. Costantini (Istituto Sperimentale per lo Studio) for helping us in Italy by providing soil samples on short notice. Nancy Mager helped make numerous text, budget and figure revisions and ensured smooth and rapid communication between the various investigators associated with this project. Rachel Oxburgh helped considerably with the modelling. Elaine Mathews and Katy Prentice provided a seemingly endless supply of answers and references to the multitude of questions raised by our research. In Kansas, we sampled the Konza Prairie, an NSF LTER site. DOE and a NASA Global Change Fellowship funded this research. We thank them all.

Table 1: Global carbon budget.

sources	1958-1978		annually for 1980's	
	GtC	Reference	GtC	Reference
fossil fuel	76	Marland & Rotty, 1984	5.4±0.5	IPCC, 1990 & 1992
deforestation	32	Houghton et al, 1990	1.6±1.0	"
total additions	108		7.0	
sinks				
atmosphere increase	43	Bolin, 1986	3.2±0.1	"
ocean uptake	28	Broecker et al 1979	2.0±0.8	"
total storage	71		5.2	
missing sink	37	(by difference)	1.8±0.4	"

Table 2: Soil Radiocarbon data for non-cultivated soils.

sampling date	R(soil)	location	vegetation/ soil type	precip. estimated (mm/yr)	temp. °C	ref
1927	0.82	Leningrad, USSR	podzol	325	7	f
1959	0.90	Amazon basin	ultisol	1500	30	f
1956	0.88	New Zealand	silt loam	1250	15	a
1959	0.93	Amador County, CA	temperate forest	250	12	n
1960	0.95	Judgeford, New Zealand	silt loam	1250	15	l
1962*	0.89	Saskatchewan, Canada	cherozemic	325	7	e
"	0.96	"	"	"	"	e
1963	1.01	Judgeford, New Zealand	silt loam	1250	15	l
1964	1.02	"	"	"	"	l
1965	1.00	"	"	"	"	l
1965	1.05	"	"	"	"	l
1966	1.07	"	"	"	"	l
1967	1.08	"	"	"	"	l
1968	1.11	"	"	"	"	l
1969*	1.01	Saskatchewan, Canada	cherozemic	325	7	d
"	0.99	"	"	"	"	d
1970	1.12	"	"	"	"	i
1970	1.07	"	"	"	"	i
1970	1.04	"	"	"	"	i
1970	1.06	"	"	"	"	i
1971	1.12	"	"	"	"	j
1971	1.03	"	"	"	"	j
1971	1.03	"	"	"	"	j
1971	1.12	"	"	"	"	l
1973	1.13	"	"	"	"	l
1977	1.09	"	"	"	"	g
1977	1.19	"	"	"	"	g
1984*	1.13	Wohldorf, FRG	hapludalf	650	8	b
"	1.12	Ohlendorf, FRG	"	"	"	b
"	1.12	Timmendorf, FRG	hapludalf	"	"	b
"	1.11	Akka, Israel	polloxevert	620	18	b
"	1.11	Qedema, Israel	"	"	"	b
"	1.12	Patancheru, India	rhodustalf	1300	27	b
1984*	1.09	Lodi, Italy	grassland	600	14	m
1985	1.22	Saskatchewan, Canada	grassland	325	7	m
1991	1.15	Konza Prarie, Kansas	grassland	732	13	m
1991	1.12	Durham, NC	deciduous	1100	15	m

Dates followed by an a are the actual dates the soil was collected. Those sampling dates followed by a have been estimated, subtracting 5 years from the publication date. We define pre-bomb as being earli than 1963. References: a(O'Brien, 1986); b(Scharpenseel et al., 1989); d(Martel & Paul, 1974b); e(Campbell et al., 1967); f(Trumbore et al., 1990); g(O'Brien, 1984); i(Goh, et al., 1976); j(Goh et a 1977); l(O'Brien & Stout, 1978); m(this study) and n(Trumbore, 1992). In Kansas, we sampled the Konza Prairie, an NSF LTER site.

Table 3: Deep soil radiocarbon values.

soil type	depth(cm)	R(soil)	location	reference
Mollisol	65-105	0.49	China	Becker-Hiedmann et al, 1987
Mollisol*	40-50	0.76	New Zealand	O'Brien, 1986
Vertisol	60-140	0.60	Israel	Scharpenseel and Becker-Heidmann, 1989
Udic	60-140	0.60	Patancheru, India	Becker-Heidmann, 1989
Mollisol	85-110	0.62	Hildesheim, FRG	Tsutsuki et al., 1987
Mollisol	80-100	0.71	"	"

*under house.

Table 4: Soil organic carbon inventories, GtC (Schlesinger, 1991). We subtract accumulating ecosystems, whose carbon turnover is very slow, from the total soil carbon inventory to gain a more accurate estimate of the global fast carbon pool.

Reservoir	Carbon inventory (GtC)
total soil organic carbon	1500
inactive soils (boreal, tundra, alpine, swamp)	500
active soils	1000
fast pool	450
slow pool	550

Table 5: Carbon inventory increases.

carbon pool	inventory size (GtC)	residence time (years)	increase, 1850-1985 (%)	carbon stored: 1850-1985 (GtC)	1958-1978 (GtC)	ann/80's (GtC/yr)
fast soil	450	25	5.3	24	7	0.6
litter,fine roots	110	3	7	7	3	0.3
long-lived vegetation	500	63	3.5	18	5	0.4
short-lived vegetations	90	1.5	8.5	8	2	0.2
total				57	17	1.5
missing sink				105	23*-37	1.8

*The missing sink decreases to 23 GtC from 1958 to 1978 if Siegenthaler and Oeschger's (1987) estimates of biospheric release are used.

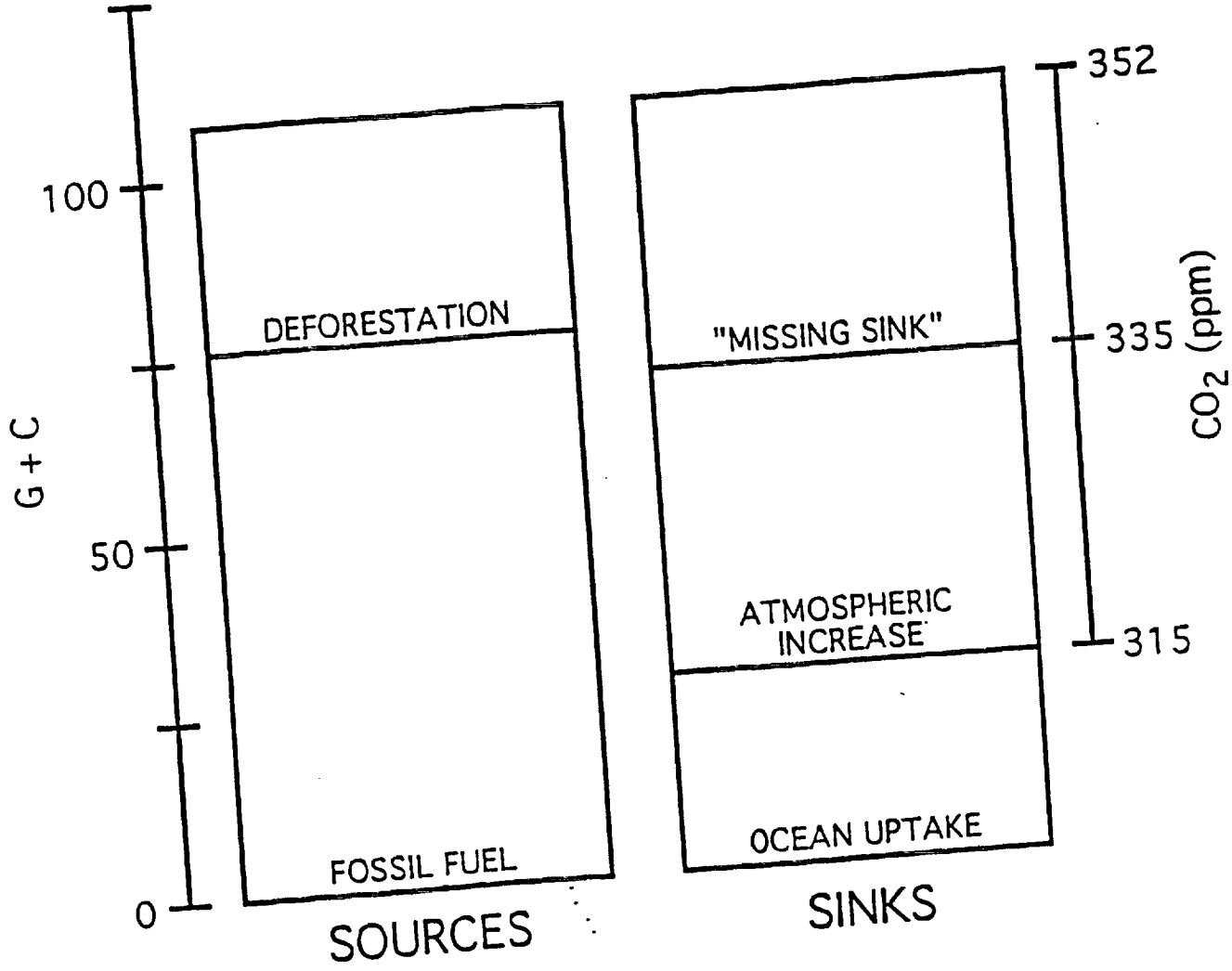

Figure 1: Title: Missing carbon sink, 1958-1978

Sources (fossil fuel and deforestation) and sinks (ocean uptake, atmospheric increase and "missing") for atmospheric carbon dioxide from 1958 to 1978. The left axis units are GtC(10^{15} grams C) and the right axis units are ppm CO_2. The fossil fuel and deforestation exceed ocean uptake and the atmospheric increase by 37 GtC. Hence, the atmosphere increased from 315 ppm in 1958 to only 335 ppm in 1978. Were the carbon in the missing sink to have remained airborne, the CO_2 content in 1978 would have been 352.

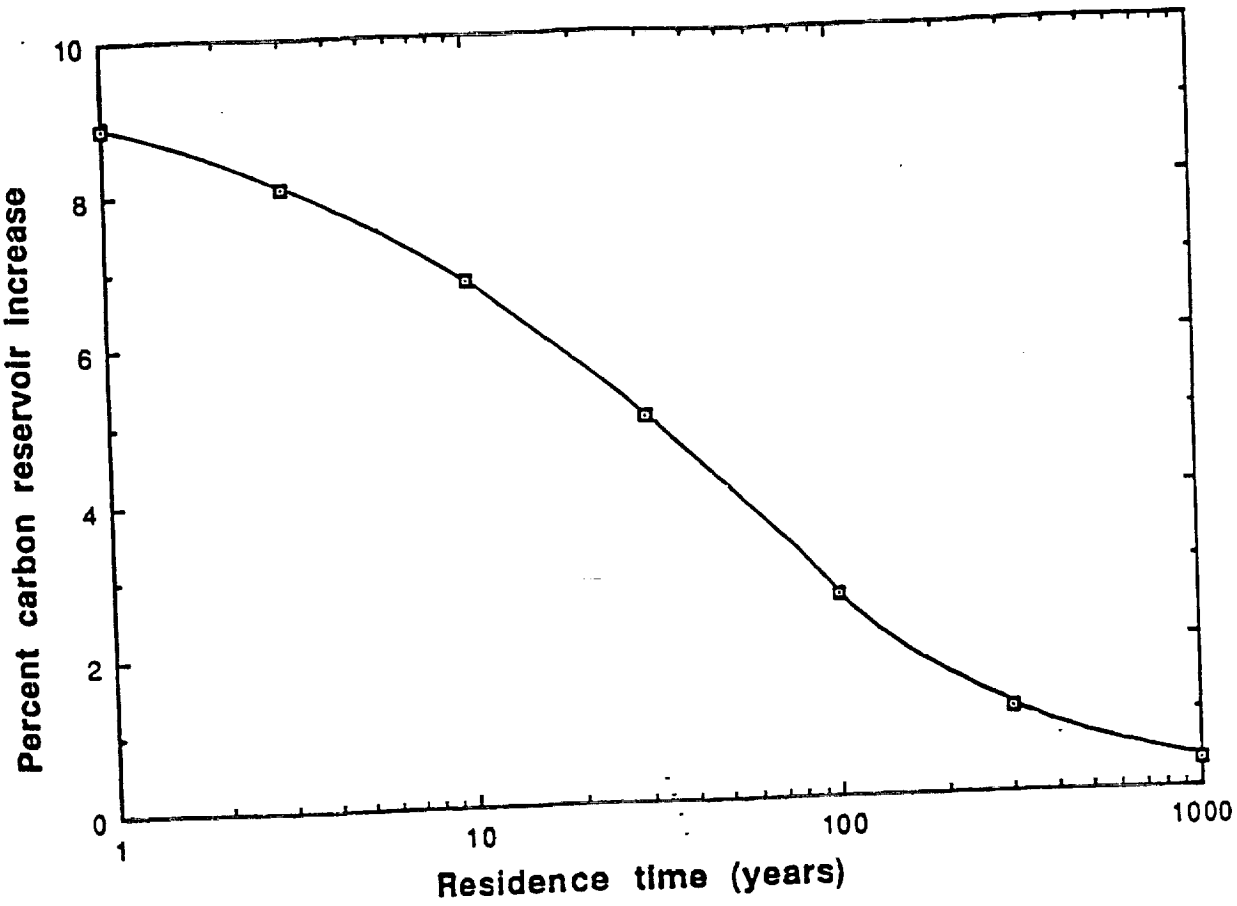

Figure 2: Title: Soil carbon residence time vs percent carbon reservoir increase, 1850 to 1985

This plot shows how residence time influences the percentage increase in the carbon inventory for a 0.35 CO_2 fertilization factor. The shortest cycling time carbon pools have the greatest increase.

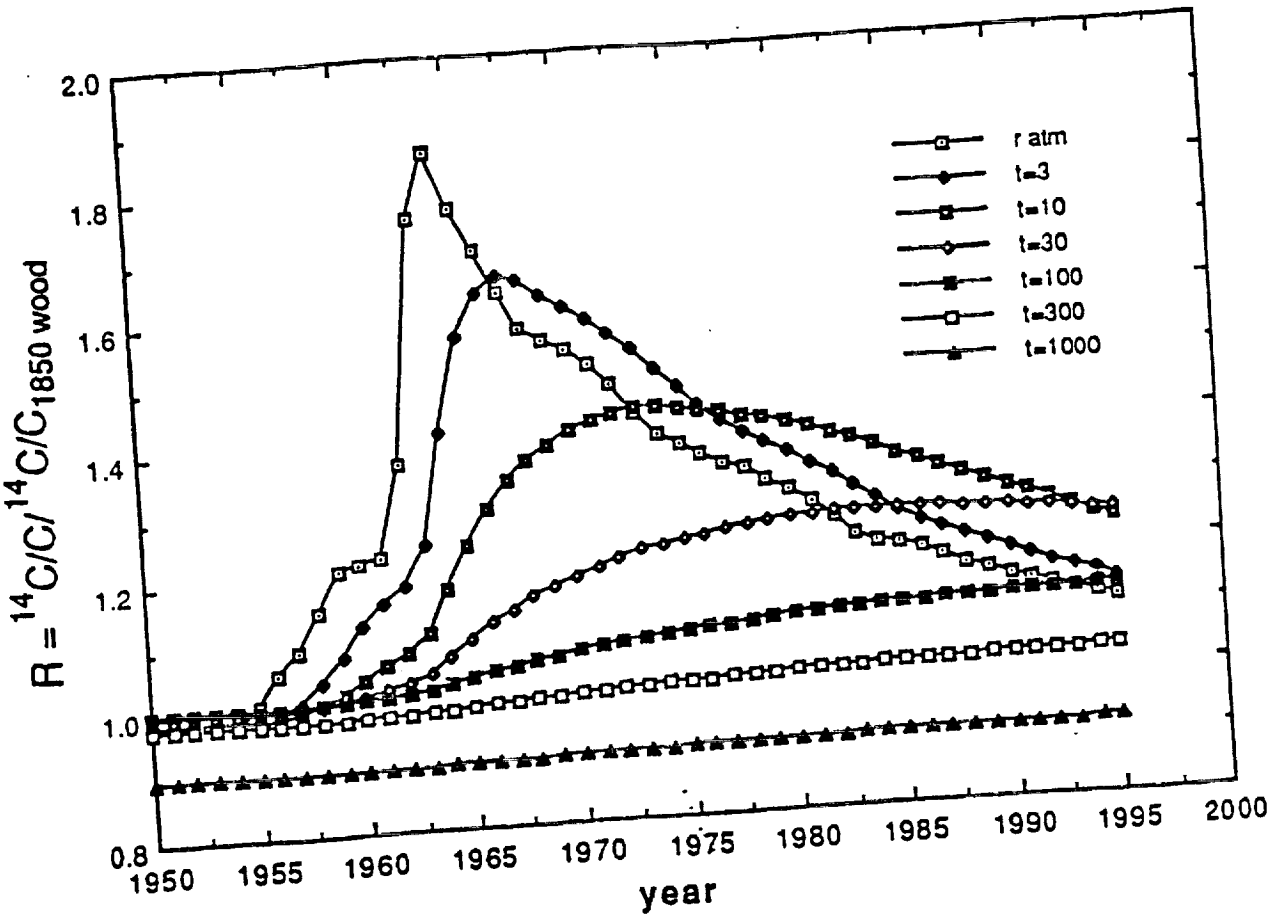

Figure 3: Title: Radiocarbon spectrum plot

C-14 ratio is plotted against time, from 1950 to 1995. The ratio ranges from 0.8 to almost 1.9. The atmospheric ratio shows the greatest increase, which stems from nuclear testing in the atmosphere. This bomb spike is propagated through the soil carbon having different residence times. The shortest soil carbon residence time plotted, 3 years, shows the greatest perturbation. However, even in this short residence time, the atmospheric signal is significantly attenuated. The longest residence time of 1000 years shows the least

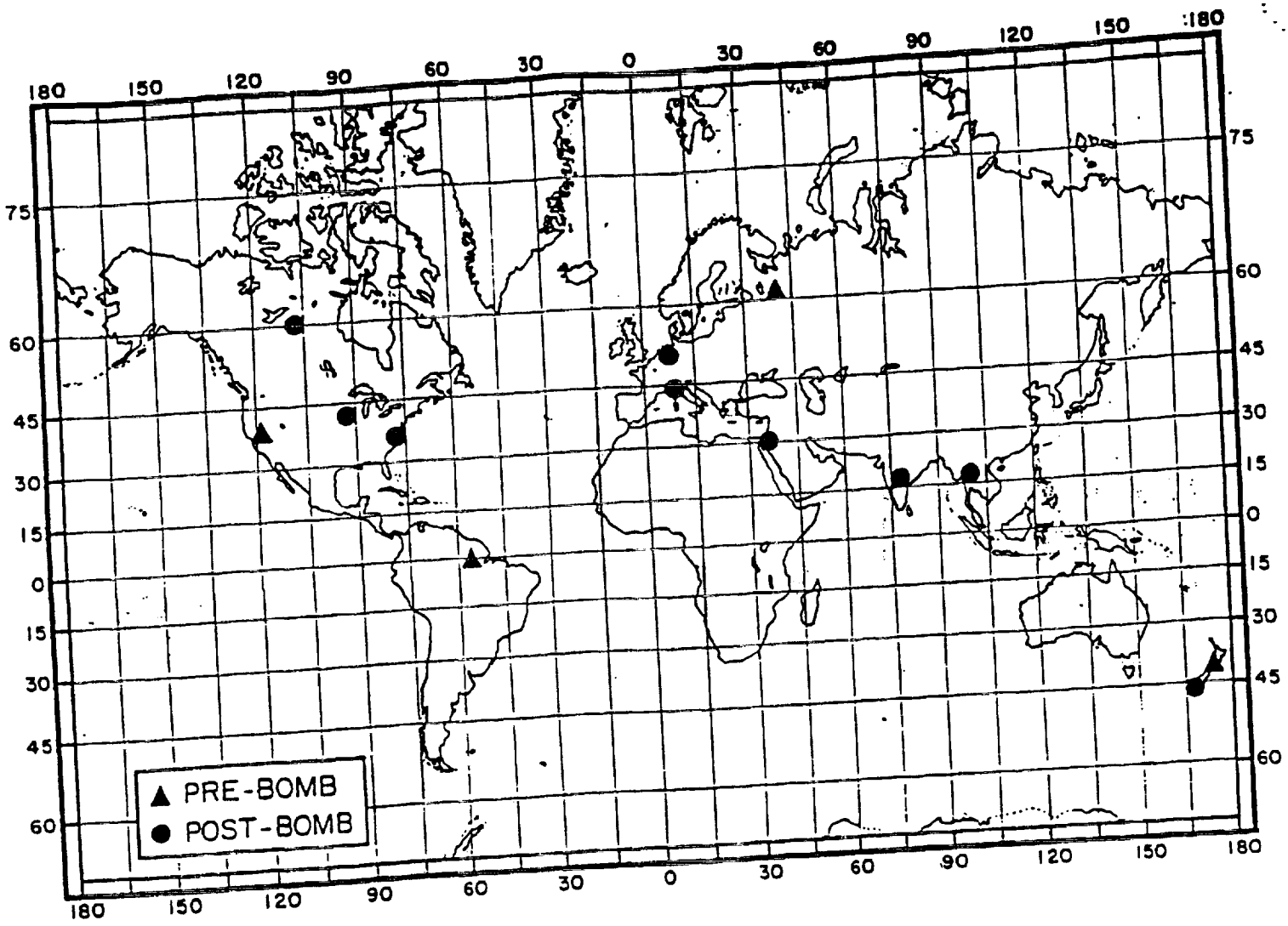

Figure 4: Title: Radiocarbon sampling site locations

The open triangles correspond to sites sampled before 1963 and the solid circles correspond to sites sampled in 1963 and later.

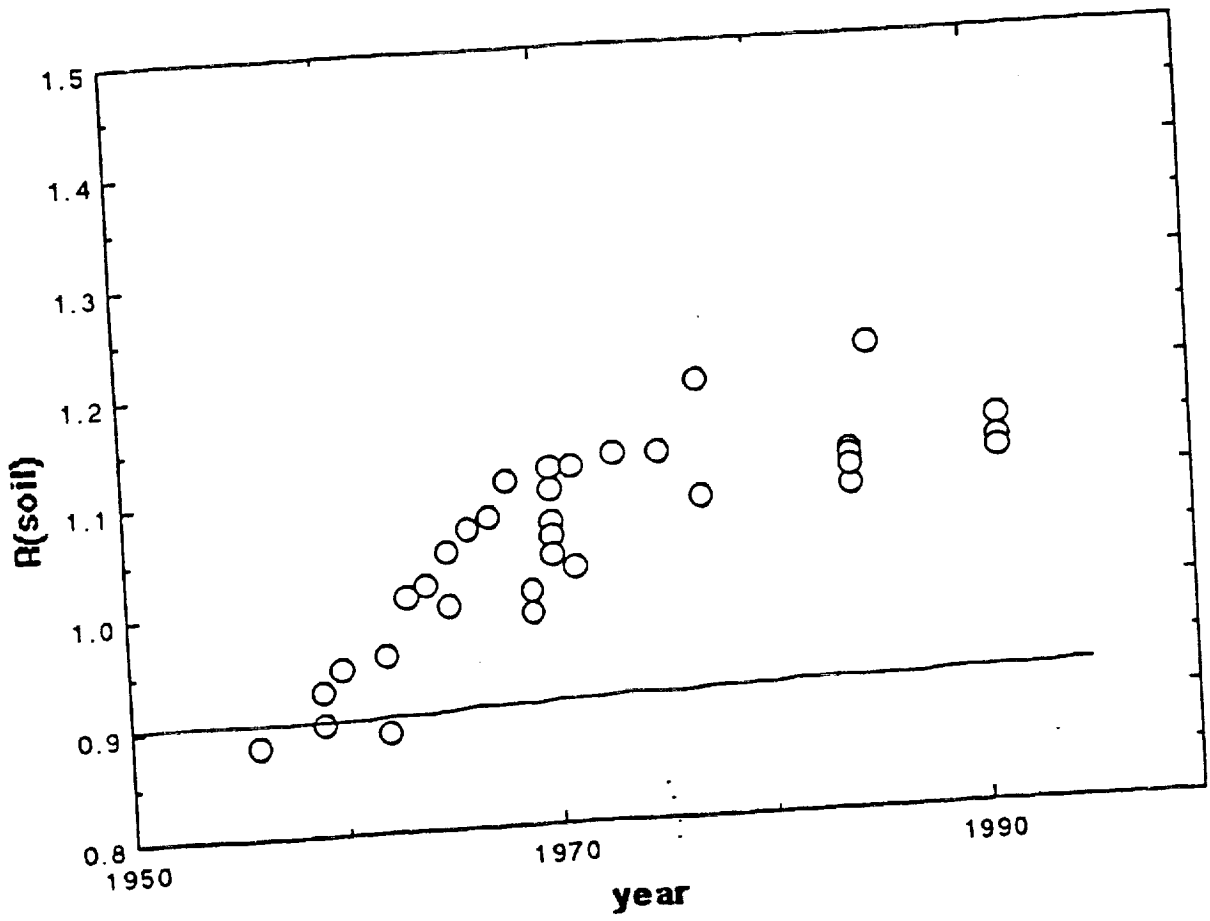

Figure 5: Title: R(soil) vs time

Measured R(soil) carbon values for non-cultivated soils are plotted against time from 1950 to 1991. The values tend to increase during the 1960's and then level off. Model results for a theoretical carbon pool having an 850-year residence time are shown by the line. If soil carbon consisted of components having this single residence time, one [illegible] to fall around this line.

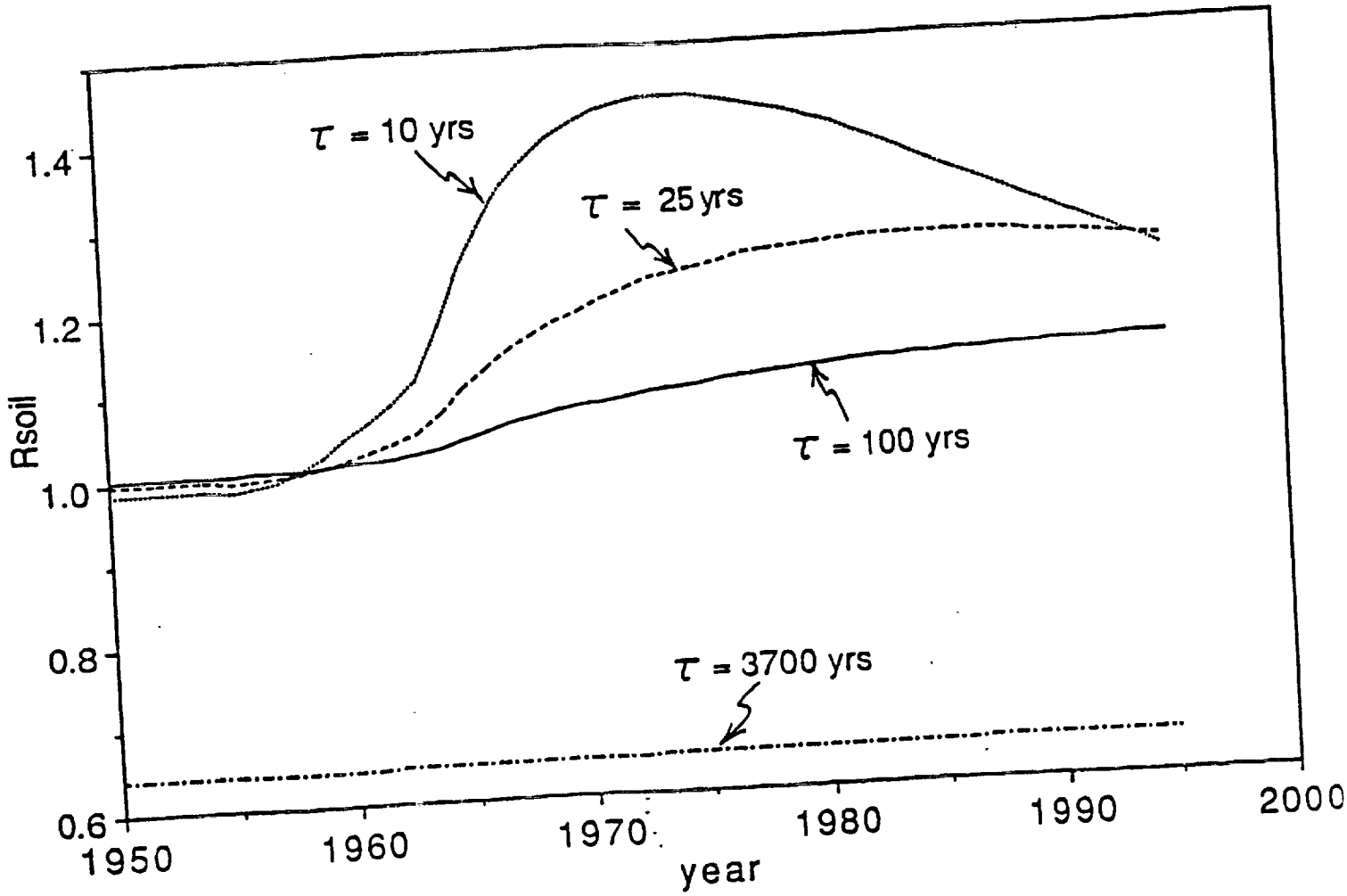

Figure 6: Title: R(soil) having residence times of 3700, 100, 25 and 10 years vs time

Soil radiocarbon values can be modeled as a system consisting of slow and fast components. We use an average deep R(soil) of 0.63 (3700 years) to estimate the residence time of the slow cycling component. We believe the fast-cycling component's reservoir is made up of components with residence times ranging from 10 to 100 years.

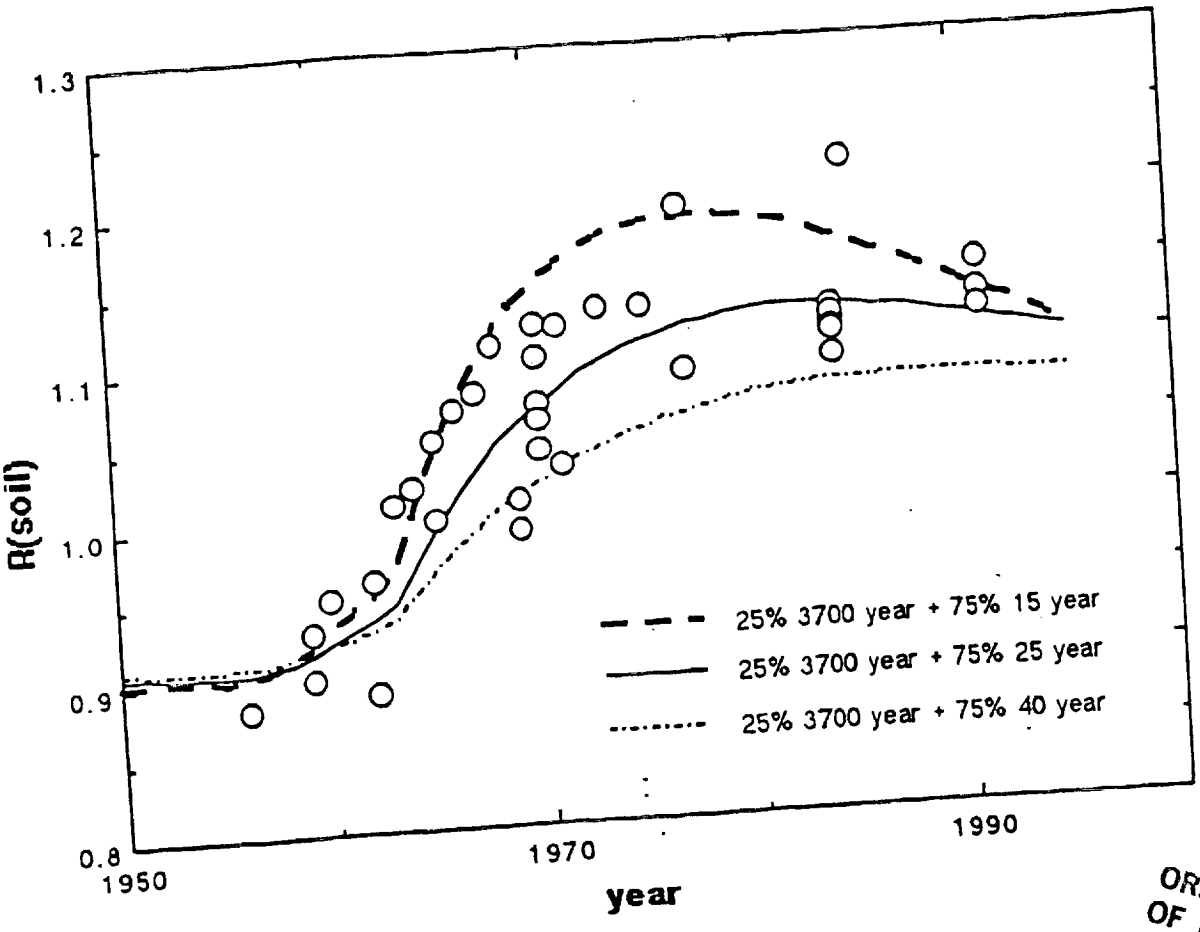

Figure 7: Title: R(soil) model predictions and R(soil) observations vs time

We combine 75% of the fast-cycling components with 25% of the slow-cycling components to reproduce pre-bomb values. The pre-bomb values for the fast-cycling pools converge because their turnover time is much less than the mean life of radiocarbon. However, these curves diverge when bomb radiocarbon is released to the atmosphere. R(soil) carbon for non-cultivated soils is also plotted (open circles). We have superimposed our soil carbon modeling results for 15-, 25- and 40-year residence times [illegible] bracket the experimental data.

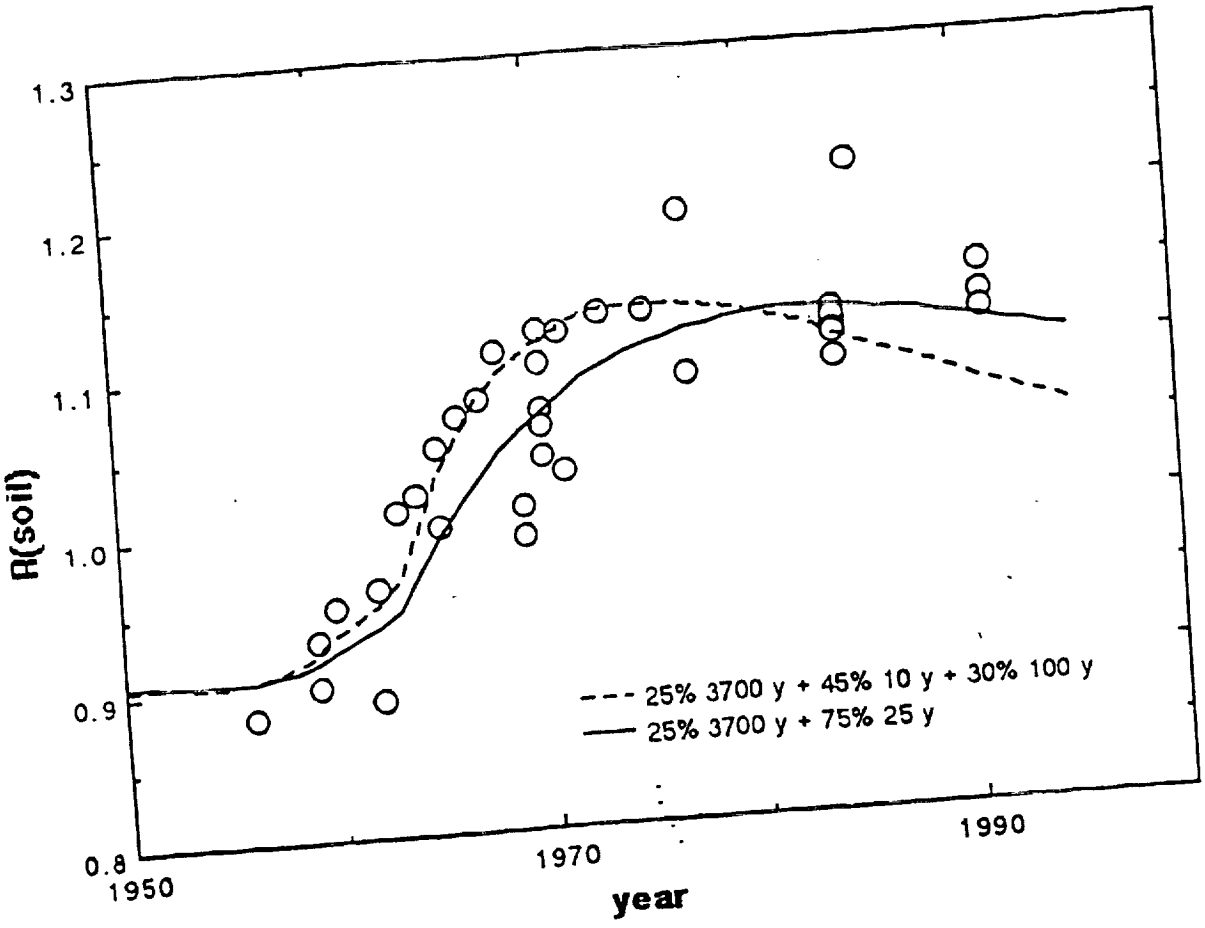

Figure 8: Title: Comparison of single fast pool with a two-component fast pool predictions.

We compare the result of the model calculation for our standard two-component mixture (25% 3700-year and 75% 25-year, case 1) with that for a three-component mixture consisting of 25% 3700-year, 45% 10-year and 25% 100-year.

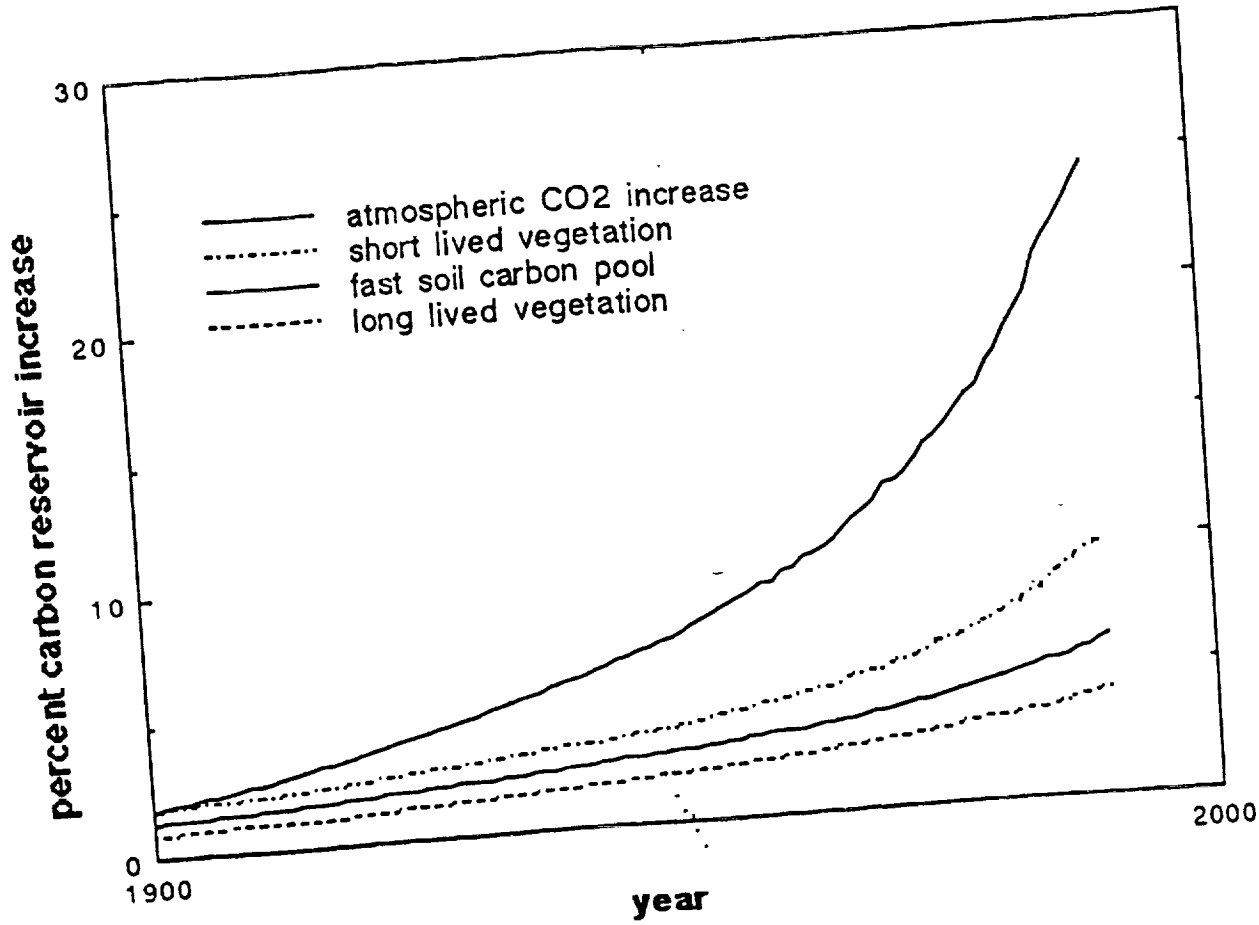

Figure 9: Title: Percent carbon reservoir increase for various carbon pools.

We plot the percent reservoir increase from 1900 to 1990 for atmospheric CO_2 observations, short-lived vegetation, fast soil and long-lived vegetation.

REFERENCES

Bacastow, R. and A. Bjorkstrom, Comparison of ocean models for the carbon cycle, in *Carbon Cycle Modelling, Scope 16*, edited by B. Bolin, pp. 29-79, Wiley, New York, 1981.

Bacastow, R. and C.D. Keeling, Atmospheric carbon dioxide concentration and the airborne fraction, in *Carbon Cycle Modelling, Scope 16*, edited by B. Bolin, pp. 103-112, Wiley, New York, 1981.

Bazzaz, F.A. and E.D, Fajer. Plant life in a CO2-rich world. *Scientific American*, January 1992, 68-74.

Becker-Heidmann, P., Liu Liang-wu, H.W. Scharpenseel, Radiocarbon dating of organic matter fractions of a Chinese mollisol. *Z. Pflanzenernahr. Bodenk., 151*, 37-39, 1988.

Becker-Heidmann, P. and H.W. Scharpenseel, Carbon isotope dynamics in some tropical soils. *Radiocarbon, 31*, 3, 672-679, 1989.

Bolin, B., How much CO2 will remain in the atmosphere? in *The Greenhouse Effect, Climate Change, and Ecosystems, Scope 29*, edited by B. Bolin, B.R. Doos and J. Jager, pp. 93-155, John Wiley, New York, 1986.

Broecker, W. S., T. Takahashi, H. J. Simpson, and T. H. Peng, Fate of fossil fuel carbon dioxide and the global carbon budget. *Science, 206*, 409-418, 1979.

Campbell, C.A., E.A. Paul, D.A. Rennie and K.J. McCallum, Applicability of the carbon-dating method of analysis to soild humus studies. *Soil Science, 104*, 3, 217-223, 1967.

Duce, R.A., P.S. Liss, J.T. Merrill, et al., Atmospheric input of trace species to the world oceans. *Global Biogeochemical Cycles, 5*, 3, 193-259, 1991.

Esser, G., Sensitivity of global carbon pools and fluxes to human and potential climate impacts, *Tellus, 39B*, 245-260, 1987.

Goh, K.M, T.A. Rafter, J.D. Stout and T.W. Walker, Accumulation of soil organic matter and its carbon isotope content in a chronosequence of soils developed on aeolian sand in New Zealand. *J. Soil Science, 27*, 89-100, 1976.

Goh, K.M., J.D. Stout and T.A. Rafter, Radiocarbon enrichment of soil organic fractions in New Zealand soils. *Soil Science, 123*, 6, 385-390, 1977.

Houghton, J. T., B. A. Callander and S. K. Varney (eds.), Climate change 1992. the supplementary report to the IPCC scientific assessment, Cambridge University Press, in press, 1992.

Houghton, J. T., G. J. Jenkins and J. J. Ephraums (eds.), Climate change. the IPCC scientific assessment, Cambridge University Press, 1990.

Houghton, R.A. and D.L. Skole, *The Long-Term Flux of Carbon Between Terrestrial Ecosystems and the Atmosphere as a Result of Changes in Land Use*, Carbon Dioxide Information Analysis Center, Oak Ridge, 1990.

Jenkinson, D. S., The turnover of organic carbon and nitrogen in soil, *Phil. Trans. R. Soc. Lond., B, 329*, 361-368, 1990.

Kauppi, PE, K Mielikainen and K Kuusela, Biomass and carbon budget of European Forests, 1971-1990. *Science, 256*, 70-74, 1992.

Keeling, Charles D., The carbon dioxide cycle: reservoir models to depict the exchange of atmospheric carbon dioxide with the oceans and land plants, in *Chemistry of the Lower Atmosphere*, edited by S. Rasool, 251-329, Plenum, New York, 1973.

Keeling, Charles D., R.B. Bacastow, A.F. Carter, S.C. Piper, T.P. Whorf, M. Heimann, W.G. Mook and H. Roeloffzen, A three-dimensional model of atmospheric CO_2 transport, 1. Analysis of Observational Data, in *Aspects of Climate Variability in the Pacific and Western Americas, Geophysical Monograph 55*, edited by David H. Peterson, pp. 165-236, AGU, Washington, D.C., 1989a.

Keeling, Charles D., Stephen C. Piper and Martin Heimann, A three-dimensional model of atmospheric CO_2 transport based on observed winds, 4. Mean annual gradients and interannual variations, in *Aspects of Climate Variability in the Pacific and the Western Americas, Geophysical Monograph 55*, edited by David H. Peterson, AGU, Washington, D.C., 1989b.

Kohlmaier, G. H., E-O. Sire, A. Janecek, C. D. Keeling, S. C. Piper and R. Revelle, Modelling the seasonal contribution of a CO2 fertilization effect on the terrestrial vegetation to the amplitude increase in atmospheric CO2 at Mauna Loa Observatory, *Tellus, 41B*, 487-510, 1989.

Maier-Reimer, E. and K. Hasselmann, Transport and storage of CO2 in the ocean -- an inorganic ocean-circulation carbon cycle model, *Climate Dyn., 2*, 63-69, 1987.

Marland, G.R. and R.M. Rotty, Carbon dioxide emissions from fossil fuels: a procedure for estimation and results for 1950-1982, *Tellus, 36B*, 232-262, 1984.

Martel, Y.A. and E.A. Paul. Use of radiocarbon dating of organic matter in the study of soil genesis. *Soil Sci. Soc. Amer. Proc., 38*, 501-506, 1974.

McGuire, A. D., J. M. Melillo, L. A. Joyce, D. W. Kicklighter, A. L. Grace, B. Moore III, and C. J. Vorosmarty, Interactions between carbon and nitrogen dynamics in estimating net primary productivity for potential vegetation in North America, *Global Biogeochemical Cycles, 6*, 101-124, 1992.

Neftal, A. et al. Ice core sample measurements give atmospheric CO2 content during the past 40,000 years. *Nature, 295*, 220-223, 1985.

Norby, R. J., C. A. Gunderson, S. D. Wullschleger, E. G. O'Neill and M. K. McCracken, Productivity and compensatory responses of yellow-poplar trees in elevated CO2, Nature, 357, 322-324, 1992.

O' Brien, B.J.and J.D. Stout. Movement and turnover of soil organic matter as indicated by carbon isotope measurements. *Soil Biol. Biochem., 10*, 309-317, 1978.

O'Brien, BJ. Soil organic carbon fluxes and turnover rates estimated from radiocarbon enrichments. *Soil Biol. Biochem., 16*, 2, 115-120, 1984.

O'Brien, B.J. The use of natural and anthropogenic C-14 to investigate the dynamics of soil organic carbon. *Radiocarbon, 28*, 2A, 358-362, 1986.

Oeschger, H., U. Siegenthaler, U. Schotterer and A. Gugelmann, A box diffusion model to study the carbon dioxide change in nature, *Tellus, 27*, 168-192, 1975.

Parton, W.J., D.S. Schimel, C.V. Cole, and D.S. Ojima, Analysis of factors controlling soil organic matter levels in Great Plains Grasslands, *Soil Science America Journal, 51*, 1173-1179, 1987.

Parton, W.J. , J. W. Stewart and C. V. Cole, Dynamics of C, N, P and S in grassland soils: a model, *Biogeochemistry, 5*, 109-131, 1988.

Peng, T.-H., Uptake of anthropogenic CO2 by lateral transport models of the ocean based on the distribution of bomb produced C-14, *Radiocarbon, 28*, 2A, 363-375, 1986.

Sarmiento, J.L. and E.T. Sundquiest. Revised budget for the oceanic uptake of anthropogenic carbon dioxide. *Nature, 356*, 589-593, 1992.

Scharpenseel, H.W. and P. Becker-Heidmann, H.U. Neue and K. Tsutsuke. Bomb-carbon, C-14 dating and C-13 measurements as tracers of organic matter dynamics *The Science of the Total Environment, 81/82*, 99-110, 1989.

Scharpenseel, H.W. and P. Becker-Heidmann. Shifts in C-14 patterns of soil profiles due to bomb carbon. *Radiocarbon, 31*, 3, 627-636, 1989.

Schlesinger, W. H. *Biogeochemistry: An Analysis of Global Change*. Academic Press, New York, 1991.

Schoenau, J. J. Nutrient cycling processes in prairie and boreal forest soils. University of Saskatchewan, Ph. D. Thesis, 1988.

Siegenthaler, U. and H. Oeschger, Biospheric CO2 emissions during the past 200 years reconstructed by deconvolution of ice core data, *Tellus, 39B*, 140-154, 1987.

Toggweiler, J.R., K. Dixon, and K. Bryan, Simulations of radiocarbon in a coarse resolution world ocean model 1. steady state pre-bomb distributions, *J. Geophys. Res, 94*, 8217-8242, 1989a.

Toggweiler, J.R., K. Dixon, and K. Bryan, Simulations of radiocarbon in a coarse resolution world ocean model 2. distributions of bomb-produced carbon-14, *J. Geophys. Res, 94*, 8243-8264, 1989b.

Trumbore, Susan. Radiocarbon measurements and soil carbon turnover rates. *Ecological Applications*, submitted.

Trumbore, Susan E., G. Bonani and W. Wolfi. The rates of carbon cycling in several soils from AMS C-14 measurements of fractionated soil organic matter, in *Soils and the Greenhouse Effect*, edited by A.F. Bouwman, pp. 407-414, John Wiley, New York, 1990.

Tsutsuki, K. et al., Investigation on the stabilization of the humus in mollisols. *S. Pflanzenernahr. Bodenk., 151*, 87-90, 1988.

Warneck, P., Chemistry of the natural atmosphere, Academic Press, New York, 1988.

Evidence for massive discharges of icebergs into the glacial Northern Atlantic

Gerard Bond*, Hartmut Heinrich+, Sylvian Huon#, Wallace Broecker*, Laurent Labeyrie**, John Andrews‡, Jerry McManus*, Silke Clasen††, Kathy Tedesco‡, Ruediger Jantschik†, and Millie Klas*

*Lamont-Doherty Geological Observatory, Palisades, New York 10964, USA
+Bundesamt fur Seeschiffahrt und Hydrographie, Postfach 30 12 20, 2000 Hamburg 36, Germany
#Department de Mineralogie, 13 rue des Maraichers, CH-1211 Geneve 4, Switzerland
**C.F.R.. Laboratoire mixte CNRS-CEA, Domaine du C.N.R.S., 91198., Gif-sur-Yvette Cedex, France
‡Institute of Arctic and Alpine Research and Geological Sciences, Box 450,University of Colorado, Boulder, Colorado 80309 USA
††Inst. und Museum fur Geologie und Palaontologie Goldschmidt-Str.3 D-3450 Gottingen, Germany
†Institut de Geologie, 11 rue E. Argand, CH-2007, Neuchatel

AS first recognized by Heinrich (1988), a series of deposits rich in ice-rafted debris and unusually poor in foraminifera are present in northern Atlantic sediments of the last glacial period. Subsequent studies reveal that these deposits form a belt extending across the entire Atlantic. Within four of the deposits are layers with an unusual set of properties. Each was deposited rapidly, each contains abundant detrital carbonate, and each has clay-sized material with unusually high K/Ar ages. The evidence leads us to propose that each layer records massive discharge of icebergs originating in Canada and possibly northwestern Greenland. The deluges appear to be the product of sudden advances of ice streams onto continental shelves combined with cooling of North Atlantic surface water. The catastrophic events may have been a consequence of dramatic cooling events or stochastic surging of the Laurentide-northern Canadian ice sheets.

To date, the most detailed study of the sediment composing the Heinrich layers has been made on cores from DSDP site 609 (Fig 1). Zones of unusually high percentages of IRD (ice-rafted detritus) and low amounts of forams clearly define the six Heinrich deposits of the last glacial period (Fig. 2). By direct AMS C^{14} dating we have confirmed the ages Heinrich (1988) inferred from oxygen isotope stratigraphy for the first three layers (~14,500, ~21,000 and ~28,000 years), and by extrapolating C^{14}-based sedimentation rates we have estimated the ages for the remaining 3 layers (~40,000, ~50,000 and ~60,000 years; Fig. 1). AMS radiocarbon ages nearly identical to those in DSDP 609 have been obtained for layers 1 and 2 in Vema core 23-16 and in core HU 75 55 from the Labrador Sea (Fig. 1; Table 1).

At DSDP site 609 four of the Heinrich deposits (1, 2, 4 and 5) contain a prominent layer that is less transparent to X-rays than the adjacent sediment. Grain counts of the > 63 μ lithic fraction in these four layers revealed a surprisingly large amount of detrital carbonate, ranging from 20% to 30% (Fig. 1). The detrital carbonate grains are rounded to subrounded and have fine-grained recrystallized textures. A few contain oolites and fragments of echinodems. Petrographic examination of the < 63 μ fraction indicates that from 40% to 60% of the identifiable material is also detrital carbonate, its abundance probably accounting for the distinctive appearance of the layers in X-radiographs. In contrast, the mineralogical composition of the other two Heinrich deposits is similar to that of the ambient sediment, consisting of 60% to 90% quartz and feldspar, variable amounts of black volcanic glass, minor amounts of mafic grains, and less than 8% detrital carbonate (Fig. 2).

Additional information has been obtained from the original suite of Dreizack seamount cores studied by Heinrich (1988). Line counts of the > 63 micron fraction

reveal the same unusual abundance of detrital carbonate in layers 1, 2, 4 and 5 as at DSDP site 609 (Fig. 2). These layers also have unusually low porosities, averaging about one half that of typical deep sea muds. Perhaps the most startling result from these cores is that in all four layers with detrital carbonate the <2μ fraction has an average K/Ar age of 897 ± 15 Ma, contrasting sharply with average ages of 442 ± 8 Ma for the < 2μ ambient sediment (Fig. 2).

Petrographic analyses of Heinrich layers in a number of Lamont piston cores constrain the distribution of the detrital carbonate IRD to a belt crossing the Atlantic between about 45°N and 52°N (Fig. 1), essentially the same area of high IRD accumulation previously identified by Ruddiman (1977). Within this belt, the thicknesses of the carbonate-rich layers increase markedly to the west (Fig. 1). In cores from the Labrador Sea, Andrews and Tedesco (in review) and Tedesco and Andrews (1992), documented even thicker equivalents of the carbonate IRD in layers 1 and 2, and they concluded that the source of the detrital carbonate must have been nearby limestone and dolomite bedrock in Hudson Strait (Fig. 2). Similar carbonate rocks are widespread in eastern Canada and northwest Greenland (Fig. 1), and they overlie a crystalline basement with ages old enough to be the source of the high K/Ar ages in the carbonate IRD in the open ocean. Thus, the Labrador Sea must have been one of the principal routes through which icebergs carrying this distinctive sediment entered the North Atlantic.

Two other features of the Heinrich deposits are worthy of mention. First, the layers with abundant carbonate IRD must have been deposited rapidly relative to the ambient sediment. X-radiographs of cores from DSDP site 609 and the Dreizack area indicate that each layer has a sharp base in distinct contrast to the gradational bases of all other IRD layers observed to the depth of the 5/6 boundary. In addition, the flux of lithic grains in the carbonate IRD layer in H2 (the only detrital carbonate layer in which we can

make a flux estimate so far), was much higher than that of the sediment on either side (Table 2). Although we have found evidence of dissolution of forams in H3 and H6, forams in the layers with carbonate IRD are well-preserved, and dissolution does not affect our estimates of shell rain-rate or faunal composition.

Second, all six of the Heinrich deposits formed during extreme climatic conditions. In DSDP site 609 and in the Dreizack area (Heinrich, 1988), the low foraminiferal layers are dominated by especially large abundances of the polar planktonic foram *N. pachyderma* (l.c) (Fig. 2; Heinrich, 1988), indicating the presence of polar-like surface water. In Vema core 23-82 in the northeastern Atlantic (Fig. 2), stages 2 through 4 contain several intervals with nearly 100% *N. pachyderma* (l.c.) and nearly 0% coccoliths, indicating extreme southward penetration of polar water (McIntyre et al., 1972). We found that three of these intervals contain carbonate IRD and are directly correlative with H2, 4 and 5. Approximate ages of the other three (McIntyre et al., 1972) are comparable to the ages of H1, 3 and 6. Our estimates of lithic and foram fluxes in DSDP site 609 also indicate that the flux of foraminifera > 150 μ dropped markedly during formation of the first three low foram zones (Table 2). Further evidence of changes in surface water comes from $\delta^{18}O$ measurements made at Gif on *N. pachyderma* (l.c.). Corresponding precisely to the carbonate rich IRD in H1 and H2 and the low foram sediment in H3 are sharp decreases in $\delta^{18}O$ of ~1 per mil (Fig. 2). As the foram abundances dictate cold conditions, these results suggest that sea surface salinities dropped during deposition of all three layers.

Based on the evidence summarized above, there can be no question that the carbonate-rich IRD in the four Heinrich layers has a very unusual origin. Any explanation based solely on North Atlantic oceanic circulation

would seem difficult to reconcile with the presence of the carbonate-rich layers in the Labrador Sea. The evidence in hand leads us to propose a tentative scenario for their origin that incorporates both oceanic circulation and events in continental ice sheets. During each of the periods of cool surface water and reduced productivity coinciding with H1, 2, 4 and 5, at least parts of the ice sheets in eastern and northern Canada and possibly in northwestern Greenland as well advanced, increasing the length of the ice fronts in contact with the ocean. This increased the numbers of icebergs breaking away from ice streams that had flowed over carbonate bedrock, leading to the release of large amounts of carbonate-bearing glacier ice into the Labrador Sea. Because of the cold sea surface temperatures, melting of this ice was slowed and the icebergs drifted into the North Atlantic. Rapid transit of large amounts of this ice eastward led to rapid deposition of carbonate-rich IRD in a wide belt reaching completely across the ocean. We have no ready explanation for the lack of abundant detrital carbonate in H3 and H6. It could be due to less extensive advances of the Canadian-northwest Greenland ice fronts or to somewhat warmer sea surface temperatures melting away the sediment-rich basal layers of icebergs near their sources.

Massive discharges of glacial ice might also explain the sudden lowering of surface salinities implied by the $\delta^{18}O$ data. The huge amount of ice drifting across the North Atlantic must have produced a large volume of meltwater. Assuming a $\delta^{18}O$ of -35 ‰ for glacial ice (Dansgarrd et al. 1982), the ~ 1 ‰ $\delta^{18}O$ change for the first three layers requires mixing only about 1 part iceberg meltwater with about 30 parts seawater. If this is correct, large amounts of glacial ice must have been drifting across the North Atlantic at the time of H3. It is interesting that the salinity drop corresponding to the ~ 1

‰ $\delta^{18}O$ decrease in all three layers is probably enough to shut down the North Atlantic's thermohaline circulation.

An important implication of the carbonate IRD layers is that they are the marine imprint of unidentified or poorly documented advances of ice sheets in eastern North America. What might have caused the ice fronts to advance is an intriguing question. If atmospheric cooling accompanied the shift of polar water southward, the ice advances may have been forced by falling temperatures. On the other hand, as suggested by Broecker et al. (1992), the lack of evidence of marked atmospheric cooling in Greenland ice cores on the time scale of the Heinrich layers leads to a second possibility, stochastic surging of parts of the ice sheets. In either case, short episodes of cooling of North Atlantic surface water appear to have been a key condition for the massive transit of icebergs far into the eastern North Atlantic and rapid deposition of carbonate-rich IRD.

TASK A: CLIMATE AND ATMOSPHERIC MODELING STUDIES

Climate Model Development and Applications

The research conducted during the past year in the climate and atmospheric modeling programs has concentrated on the development of appropriate atmospheric and upper ocean models, and preliminary applications of these models. Principal models are a one-dimensional radiative-convective model, a three-dimensional global climate model, and an upper ocean model. Principal applications have been the study of the impact of CO_2, aerosols and the solar 'constant' on climate.

Progress has been made in the 3-D model development towards physically realistic treatment of these processes. In particular, a boundary layer, land surface and convection schemes have now been incorporated. The model containing these improvements will be run and evaluated.

A version of the climate model has been created which follows the isotopes of water and sources of water (or colored water) throughout the planet. Each isotope or colored water source is a fraction of the climate model's water. It participates in condensation and surface evaporation at different fractionation rates and is transported by the dynamics. A major benefit of this project has been to improve the programming techniques and physical simulation of the water vapor budget of the climate model. Applications include simulations of deuterium and oxygen-18 for both current climate and 18,000 years ago, the source of precipitation in each grid box in the North Hemisphere, and a stratospheric tritium experiment to simulate the atomic testing of the 1950s and 60s (Koster et al., 1990).

During the past year, papers have been published, which investigate the impact of altered ocean heat transport on climate (Rind and Chandler, 1991), and the likelihood of future drought caused by the projected increase in temperature (Rind et al., 1990).

Modeling of the climate and vegetation change of the last 30,000 years, and of the Little Ice

Age, has begun with the assistance of Rick Healy and initial attempts to compile appropriate boundary conditions for GCM runs.

Studies of the sensitivity of North Pacific sea surface temperatures (SST) to global climate change continue. A paper in preparation will detail the results of the North Pacific cooling experiment, which has significant implications for northern hemisphere temperature depression, as well as ice sheet growth.

An experiment for natural ocean variability on the decadal to millennium time scale has been conducted with a low-resolution ocean general circulation model. The model comprises a sector of 120 degrees longitude extent, with a geometry similar to that of the Atlantic ocean. The model is initially run to equilibrium for 2000 years, forced with the zonal average of climatological wind stress, surface temperature, and salinity fluxes, parameterized in terms of a relaxation term to the zonally-averaged observed climatology. During the second part of the run, the surface salinity flux is imposed as the value obtained from the last 500 years of the first part of the run. During 2000 years with salinity flux forcing, the model shows considerable variability in the decadal to millennium time scale. The evolution of the meridional mass transport, salinity, temperature, heat and salt transport have been analyzed. The empirical orthogonal functions for these variables have been obtained for > century time-scales. A transition to one-cell pole-to-pole circulation state is observed, with circulation anomalies in the deep ocean appearing in the first empirical orthogonal function. The higher modes show variability in upper levels. Dr. Z. Garraffo (Associate Research Scientist, Columbia University), has done this work in collaboration with Dr. Inez Fung (GISS), using the Goddard Space Flight Center Cray computer.

Work begun this past year with Dr. Silvia Garzoli (Lamont-Doherty Geological Observatory), on the analysis of Semter and Chervin's global ocean general circulation model has been completed and published. The model output has been completed and published. The model output has been compared with data from regions of western boundary currents, in order to establish similarities and differences with observations, that will be taken into account for further use of the model results. The analysis contains a comparison of upper model temperature fields with satellite-derived sea

surface temperatures. Empirical orthogonal functions are obtained for both model and observations, in order to reduce the dimensionality of the system; similarities and differences between model and observations are then discussed. In addition, statistical distribution functions of the observed thermal front are compared with model frontal positions. A comparison between upper ocean eddy kinetic energy predicted by the model and fields derived from GEOSTAT altimeter data and from drifting buoys has been made. The analysis was done for two western boundary current regions: the western South Atlantic and the Kuroshio-Oyashio system. In the analyzed regions, maximum temperature differences between model and observed frontal positions were found to be in the range 2 to 4 degrees. The eddy life cycle is slower in the model than in the observations. The model variability is weaker than the observed one; this difference is more pronounced in the South West Atlantic Ocean. Two papers from this study are in press in the Journal of Geophysical Research.

Paleoclimate Studies

Analysis of late-glacial pollen, macrofossil, acceleration mass spectrometry (AMS) controls and fish-scale stratigraphy from the northeastern U.S. has been concluded. The three cores analyzed indicate a sudden warming at 12,500 yr BP, followed by a Younger Dryas cooling between 11,000 and 10,000 yr BP. Subsequent warming was also rapid, occurring in less than 100 years, and at least three boreal species disappeared locally. A paper based on these findings is in preparation. Pollen and macrofossil research on two Vermont cores is still underway.

Progress on research from the southeastern United States continues. Margaret Kneller (GRA, Columbia University) has completed the pollen and macrofossil stratigraphy from a core from Brown's Pond, Virginia, which contains a 17,000 yr record. She has also completed a cross-basin transect, comparing stratigraphy and loss-on-ignition in 5 cores. She returned to the field this past summer and retrieved another core in order to examine the late-glacial interval at higher resolution. Research on the 18,000 year record from a Georgia core has also begun.

Studies of climate change at high latitudes has continued, with field work in Kodiak Island providing a detailed examination of the glacial to interglacial changes in stratigraphy, tephras, pollen,

macrofossils, and glacial history. A preliminary pollen diagram from Kodiak Island shows rapid climatic oscillations during late-glacial time. As part of the investigation, it will be determined whether or not this reversal is correlative with the Younger Dryas cooling.

Field research in Russia (July, 1991) resulted in the acquisition of four peat cores from Siberia which are being examined for vegetational and climatic change. AMS dates on these cores is approximately 9000 yr BP, near the beginning of the Holocene Epoch. Collaboration with Dr. Andre Andreev (Institute of Geography, Moscow) will result in production of a global map showing the initiation of high latitude peatland.

Ongoing studies of the origin of peatland formation in Alaska have provided AMS dates on macrofossils from permafrost peat cores. The peat formation ranges in age from 16,000 to 8,000 yr BP.

Climate Change Applications

A Coastal Hazards Data Base for the Southeast U.S. has been created to categorize and identify shorelines at high risk to future sea level rise, caused by climate warming. The data base consists of a total of 13 land, marine and climate variables. These variables have been grouped into three clusters, which, in order of importance, represent permanent inundation, episodic inundation, and erosion potential, respectively. Each data variable was assigned to one of 5 risk classes, and these were combined into a Coastal Vulnerability Index (CVI) that provides a relative measure of the risk faced by any given segment of the shoreline. Among the highest risk shorelines in this region are Cape Hatteras, North Carolina and the coast of Louisiana. At Cape Hatteras, the episodic inundation variables (mostly climate variables) contribute a significantly larger proportion to the total CVI, whereas at Caminada Pass, the permanent inundation factors (due to the anomalously high SLR) assumes a greater share of the total score. Sea level rise (SLR) scenarios, modified from the IPCC 1990 and 1992 findings, for local subsidence effects, were applied to six test-sites in the U.S., which have been selected on the basis of the CVI rating. These SLR scenarios were utilized to calculate the extent of inundation under various shoreline response models, as documented more fully in Daniels

et al. (1992).

A project was initiated to assess the importance of methane hydrate in permafrost and deep-sea sediments as a future potential source of atmospheric methane, under warmer climate conditions. In the initial phase of this study, estimates have been made of methane hydrate reservoirs in the world's oceans, based on two proposed models of hydrate formation: a) in-situ bacterial formation and b) pore fluid-migration. While both models predict similar methane volumes, their distribution of gas hydrate with respect to the sub-seafloor surface differs significantly in terms of the thermal response to climate warming. Since the thermal pulse from increased ocean temperatures will travel downward into the seafloor sediment, hydrates distributed uniformly with depth from the ocean bottom, as in the first case, will potentially release more methane within the next 100 years, than hydrates concentrated at depth, as predicted by the second model. Further work is in progress to assess the relative merits of these two models and to calculate the thermal penetration at depth, for plausible scenarios of global temperature warming within the next 100 years.

SAGE II

In order to explore the solar cycle/tropospheric connection, several preliminary experiments have been conducted to assess the likelihood of producing a realistic response. Considering that the effect of solar activity variations is apparently observed more clearly when modulated by the phase of the Quasi-Biennial Oscillation (QBO), in the first experiment, a QBO was induced in the model, by using an additional momentum forcing in the lower stratosphere to produce either strong tropical east winds or west winds (the model under normal circumstances does not generate a QBO, perhaps because of insufficient resolution). Then a set of initial conditions (outside the tropics) which had produced a stratospheric warming in the control run was reintroduced. The model generated a strong warming in the QBO east phase, but not in the west phase. This was the result of increased upward wave activity flux from mid-latitudes during the QBO-east. The tendency for warming mainly during the east phase is in agreement with observations. The experiments suggest the model is able

to differentiate dynamic events in its different QBO phases despite the artificiality of the QBO generation.

In the next experiment, using the control run, the UV radiation below of 0.3μ was increased by 50%. This is greatly in excess of observed values (which are still somewhat uncertain) but in line with a general modeling approach: first use strong forcing to elucidate mechanisms, and see if there is any response, then reduce the forcing back to realistic magnitudes. With the increased UV heating of the ozone layer in the tropical regions receiving solar insolation, the west winds in the Northern Hemisphere increased (consistent with the thermal wind relationship). The stronger zonal winds reduced the vertical propagation of wave activity and reduced the amplitudes of planetary waves.

TASK B: CLIMATE APPLICATIONS OF EARTH AND PLANETARY OBSERVATIONS

Cloud Climatology

During the past year, the study of tropical convection using ISCCP data has continued. Examination of changes in convection both during El Nino events and between non-El Nino years shows that the nature of the shift in convective properties associated with longer time scales is not the same as the rapid variations that occur on daily to monthly time scales. Moreover, the El Nino-related changes appear similar to interannual changes. An analysis of possible feedbacks on tropical sea surface temperatures (SST) was performed to examine a hypothesis that tropical SST is controlled by convection through a local cloud-radiative feedback. The results show that the net effect of changing convective clouds on surface radiative heating is small compared with changes in evaporative cooling and that neither change is large enough to completely control the SST changes. This confirms other studies that show that El Nino SST changes are controlled more by ocean dynamics than by changes in the surface energy budget. These results have been published.

A global survey of cloud particles sizes for low-level, liquid water clouds was conducted for the four seasons, and for morning and afternoon, using multi-spectral radiance data from two polar orbiting weather satellites. Although validation data are scarce, agreement with in-situ measurements

from FIRE (First ISCCP Regional Experiment) was found to be excellent, for two cases. The results of this survey confirmed earlier aircraft results in showing that cloud droplet sizes are systematically larger in marine clouds as compared to land clouds. Moreover, a systematic hemispheric difference was found in the droplet sizes, which appears to be consistent with that predicted by the different abundances of tropospheric aerosols. A significant diurnal variation of cloud droplet size, increasing from morning to afternoon, is also found to occur in marine and land clouds at low latitudes. This study shows that the relationship of cloud particle size, optical thickness and water content is more variable than commonly assumed in most climate models. A paper based on this Ph.D. thesis research of a recently-graduated GRA is in preparation.

A study of the variations of the optical thickness of low level clouds at low and middle latitudes has been extended to a combination of satellite and surface weather observations. The earlier results, based on satellite data, have been submitted for publication. They showed that there is change in the behavior of low-level cloud optical thickness with temperature. The optical thicknesses of "cold" clouds ($T < -5°C$) increase with increasing temperatures, a rate that is proportional to the increase of the adiabatic cloud water amount in clouds. On the other hand, the optical thicknesses of "warm" clouds decrease with increasing temperatures. If this behavior also occurs during a climate warming event, then the global cloud radiative feedback is positive. The cloud-radiative feedback also varies with latitude in such a fashion as to nearly eliminate the amplification of climate change with latitude that is found in most climate models, but is not observed. The extended study addressed the question of whether these observed changes in cloud optical thickness were due to changes in cloud water content or whether they were caused by changes in cloud droplet size or vertical extent. Satellite measurements of cloud particle sizes indicate that the changes are too small to explain the observed changes in optical thickness. Combining rawinsonde and satellite data shows that vertical extent changes also do not explain the observed optical thickness changes. Moreover, the hypothesis that the change in behavior of cloud water content is associated with a change in precipitation efficiency with temperature is supported by the changing frequency

of precipitation occurrence with temperature found from surface observations. These results represent the Ph.D. thesis research of a second GRA that was successfully completed this year, and form the basis of another paper, in preparation.

New convection and cloud parameterizations for the GISS climate GCM continue to be tested by comparisons against the ISCCP data and by performing climate sensitivity studies with the climate model. One notable success is the clear improvement of the model cloud changes associated with an El Nino event (where the model is forced by the observed changes in SST) when the new convection and cloud parameterizations are used.

Comparisons of cloud water contents inferred from ISCCP cloud properties and from microwave measurements show excellent agreement for liquid water clouds (the microwave measurements are not sensitive to the ice phase), except for very low values. The microwave measurements have difficulty detecting low water contents because of uncertainties in water vapor effects; hence the optical measurements of ISCCP are more sensitive and "see" about twice as much cloud as the microwave measurements. The high resolution measurements of ISCCP can also be used to evaluate other sources of error for the microwave measurements. These results are being prepared for publication. This work represents the thesis research of a third GRA.

A climatology of cloud layer thicknesses has been obtained that is based on 14 years of rawinsonde measurements of temperature and humidity profiles from 60 northern hemisphere sites. This represents a unique dataset. Comparison of cloud statistics in this dataset with the full cloud climatology from surface observations indicates that the cloud layer climatology is generally well sampled; however, it is composed almost exclusively of cases with a single cloud layer. Analysis of the results indicates little diurnal or seasonal variation in cloud layer thicknesses but a systematic increase of thickness with latitude and altitude. However, a more thorough analysis is needed, because the results clearly depend on cloud types: the actual layer thickness distributions within each altitude range are multi-modal. The preliminary analysis of these results is being prepared for publication, based on the thesis research of a fourth GRA.

Three significant improvements have been made to the procedure for calculating global, total solar and thermal infrared fluxes at the top of the atmosphere and at the surface from the ISCCP dataset. The most important change is in the prescription of the surface albedo from the ISCCP visible reflectances: the estimated near-IR albedos for land surfaces proved to be too large when compared with ERBE observations have been calculated. A new climatology of tropospheric aerosol, with more realistic geographic variations, has been added to the radiative model. A more accurate parameterization of the angular dependence of radiative transfer through clouds has been implemented in the radiative model. All of these changes have improved the validation comparisons. Validation studies and sensitivity tests have been completed and the results are being prepared for publication. Routine calculations, to cover several years of data, have commenced. These results will be used to study cloud radiative feedbacks on synoptic, seasonal and longer-term variations.

A simpler method for calculating surface solar irradiance was developed and described in a paper (Bishop and Rossow 1991). A 7.5 year climatology of daily surface solar irradiances has been produced and is being analyzed for ocean biospheric studies.

Planetary Studies

Tracking of polarization features above the visible cloud level on Venus yields a mean zonal velocity of -23.5 m/s, which is much slower than derived from tracking of UV features near the cloud top. Preliminary estimates of haze optical depth reveal two distinct regimes: one of high haze optical depth and high variability in polar regions, and the other of lower optical depth and variability at lower latitudes.

PUBLICATIONS

(1991-1992 and in press)

Tasks A and B

Balachandran, N.K., R.A. Plumb, R.A. Suozzo and D. Rind, 1992: The QBO and stratospheric warming-model results. J. Geomag. and Geoelect. 43, 741-757.

Balachandran, N.K., and D. Rind, 1992: Effects of equatorial stratispheric winds on polar temperatures (in prep.).

Bishop, J.K.B., and W.B. Rossow, 1991: Spatial and temporal variability of global surface irradiance. J. Geophys. Res., 96, 16, 839-16, 858.

Brest, C.L., and W.B. Rossow, 1992: Radiometric calibration and monitoring of NOAA AVHRR data for ISCCP. Int. J. Remote Sensing, 13, 235-273.

Carlson, B.E., A.A. Lacis, and W.B. Rossow, 1992a: The abundance and distribution of water vapor in the Jovian atmosphere as inferred from Voyager IRIS Observations. Astrophys. J., 388, 648-668.

Carlson, B.E., A.A. Lacis and W.B. Rossow, 1992b: Ortho-para hydrogen equilibration on Jupiter. Astrophys. J., 393, 357-372.

Carlson, B.E., A.A. Lacis and W.B. Rossow, 1992c: Tropospheric gas composition and cloud structure of the Jovian North Equatorial Belt. J. Geophys. Res., (in press).

Carlson, B.E., A.A. Lacis and W.B. Rossow, 1992d: Belt-zone variations in the Jovian cloud structure. J. Geophys. Res. (submitted).

Chandler, M.A., D. Rind and R. Ruedy, 1992: Pangaean climate during the early Jurassic-simulation and the sedimentary record of paleoclimate, Geol. Soc. Am. Bull., 104, 543-559.

Daniels, R.C., Gornitz, V.M., Mehta, A.J., Lee, S.C., and Cushman, R.M., 1992: Adapting to sea-level rise in the U.S. Southeast: the influence of built infrastructure and biophysical factors

on the inundation of coastal areas, Final Report, ORNL (in press).

Fu, R., A.D. Del Genio, W.B. Rossow and W.T, Liu, 1992: Cirrus cloud thermostat for tropical sea surface temperatures tested using satellite data. Nature, (in press).

Garrafo, Z., S. Garzoli, W. Haxby, G. Podestá, O. Brown and D. Olson, 1992: Analysis of a General Circulation Model Product. AGU Ocean Science Meeting, New Orleans, January 1992.

Garrafo, Z., S. Garzoli, W. Haxby and D. Olson, 1992: Analysis of a General Circulation Model. Part 2: The distribution of kinetic energy in the South Atlantic and Kuroshio/Oyasio systems. J. Geophys. Res., (in press).

Garzoli, S., Z. Garraffo, G. Podestá and O. Brown, 1990: Analysis of General Circulation Model Product: Part I: Frontal systems in the Brazil/Malvinas and Kuroshio/Oyashio regions. J. Geophys. Res. (Accepted).

Gornitz, V., 1992: Mean Sea-Level Changes in the Recent Past, in R.A. Warrick and E. Barrow, eds., Climate and Sea Level Change: Observations, Projections and Implications, Cambridge University Press (in press).

Gornitz, V.M. and White, T.W. (contributors), and Daniels, R.C. (compiler), 1992: A Coastal Hazards Data Base for the U.S. East Coast, ORNL/CDIAC-45, NDP-043A.

Kneller, M. and D. Peteet, 1991: A Late-Quaternary record of changing depositional environment and vegetation from Virginia, as evidenced for altered climatic regimes. Geol. Soc. Am. Abstract with Programs, 23, A407.

Peteet, D.M., 1991: Postglacial history of lodgepole pine near Yakutat, Alaska. Canadian Journal of Botany 69, 786-796.

Peteet, D.M., 1992: Major contributions of radiocarbon dating to palynology: past and future. Radiocarbon, 29, 454-472.

Peteet, D.M., 1992: The palynological expression and timing of the Younger Dryas event - Europe versus Eastern North America, In: The Last Deglaciation: Absolute and Radiocarbon Chronologies, eds. Bard, Edouard and Broecker, Wallace S., Proceedings of the NATO

Advanced Research Workshop at Erice, Sicily (Italy), December 9-13, 1990. Springer-Verlag, New York, pp. 327-344.

Peteet, D.M., 1992: Book review of *Quaternary Landscapes*, eds. Linda Shane and Edward Cushing. Univ. of Minn. Press, Minneapolis, Minn. Quaternary Research (accepted).

Peteet, D.M. and Mann, D., 1992: A Late Quaternary paleoclimate record from Kodiak Island, Alaska. 22nd Annual Arctic Workshop, INSTARR, Boulder, CO, p. 113-114.

Peteet, D.M., Rind, D., and Kukla, G., 1992: Wisconsin ice sheet initiation -- Milankovich forcing, paleoclimatic data, and global climate modeling. Geological Society of America Special Paper (in press).

Reihle, J.R., Mann, D.H., Peteet, D.M., Engstrom, D., and Brew, D.A., 1992: The Mt. Edgecumbe tephra deposits: a late Pleistocene stratigraphic marker in southeastern Alaska. Quaternary Research 37, 183-202.

Rind, D., N.K. Balachandran and R. Suozzo, 1992: Climate change and the Middle Atmosphere. Part II: The impact of volcanic aerosols. J. of Climate, 5, 189-208.

Rind, D., E.-W. Chiou, W. Chu, J. Larsen, S. Oltmans, J. Lerner, M.P. McCormick and L. McMasters, 1992: Overview of the SAGE II water vapor observations: method, validation and data characteristics. J. Geophys. Res.

Rossow, W.B., and L.C. Garder, 1992: Cloud detection using satellite measurements of infrared and visible radiance for ISCCP. J. Climate, (submitted).

Tselioudis, G., W.B. Rossow, and D. Rind, 1992: Global patterns of cloud optical thickness variation with temperature. J. Climate, (in press).

TASK C: CHEMISTRY OF EARTH AND ENVIRONMENT

The Goddard Institute for Space Studies (GISS) provides funding for Lamont-Doherty Geological Observatory (LDGO) to support graduate student research in geochemistry with close ties to subjects under study by Dr. James Hansen and the Climate Modeling group at GISS. In most cases,

these projects involve use of the GISS GCM. This progress report briefly outlines the activities of eight current graduate students who are working with Professor Wallace S. Broecker, Geochemistry, at LDGO on projects related to global change.

Fritz Zaucker (GRA, LDGO) is expecting to defend his thesis on the water vapor transport through the atmosphere and its impact on ocean circulation, in the Fall, 1992. He intends to accept a NASA post-doctoral fellowship at GISS.

Kevin Harrison (GRA, LDGO) is starting his final year at Columbia University. His thesis is directed toward estimating the extent to which CO_2-induced growth enhancement has increased the inventories of carbon in soils, litter, and vegetation. A paper describing his work to date is included in Appendix A.

Jeff Severinghaus (GRA, LDGO) is just beginning his Ph.D. research. He is doing trace gas and isotope measurements in Biosphere 2 in order to document the utility of research relating materials from closed ecosystems to our understanding of terrestrial biogeochemistry. His first project is to determine the ratio of ΔCO_2 to ΔO_2 and $\Delta\delta^{13}C$ to ΔCO_2 throughout the diurnal cycle. The pCO_2 in Biosphere 2 current goes from 1300 ppm at day's beginning to 500 ppm at day's end. His second project will be to determine the Dole effect (oxygen isotope fractionation during repiration).

Roberto Gwiazda (GRA, LDGO) is in the second year of Ph.D. research. He is trying to assess the role of soil CO_2 in the rate of silicate weathering. To date, he has been doing pilot studies on small basins in the vicinity of Lamont (soil CO_2, ground water CO_2 and stream alkalinity).

Lucy Charles (GRA, LDGO) is a first year student. She has been working with Drs. Dave Archer and Taro Takahashi on mixed layer ocean chemistry modeling and with Prof. W.S. Broecker on evaluating the estimates of the northern to southern hemisphere transport of carbon in the forms of CH_4 and CO.

Jerry McManus (GRA, LDGO) is a second year student. He is working on the ice rafting record in northern Atlantic sediments. In particular, he is trying to determine the causes and effects

of large armadas of icebergs released into the Atlantic by surges of the eastern margin of the Laurentian ice sheet (see Appendix B).

Abhijit Sanyal (GRA, LDGO) is a first year Ph.D. student. He is attempting to document the extent of chemical erosion in the deep tropical Pacific during Holocene time. This study has important implications to the debate about the role of the $CaCO_3$ cycle in glacial to interglacial atmospheric CO_2 content changes.

Rachel Oxburgh (GRA, LDGO) is a second year Ph.D. student. She is trying to reconstruct oceanic osmium isotope content changes over the last 60 million years through measurements on deep-sea sediments. The purpose is to determine how global chemical weathering rates changed forty million years ago when the Himalayas were created through the collision between the Indian and Asia land masses.

PUBLICATIONS

(1991-1992 and in press)

Task C

Bond, G., W.S. Broecker, R. Lotti and Jerry McManus, 1992: Abrupt color changes in isotope stage 5 in North Atlantic deep sea cores: Implications for rapid change of climate-driven events. NATO volume (in press).

Bond, G., H. Heinrich, J. Andrews, R. Jantschik, S. Huon, J. McManus, W.S. Broecker and G. Bonani, 1992: Evidence for catastrophic discharges of glacial ice into the northern Atlantic. Nature (in press).

Broecker, W.S., 1992: Defining the boundaries of the BOA warm and YD cold isotope episodes. Quaternary Research 38, 135-139.

Broecker, W.S., 1992: Global Warming on Trial. Natural History, 4 (92), 6-14.

Broecker, W.S., 1991: The Great Ocean Conveyor. Oceanography, 79-89.

Broecker, W.S., 1991: Keeping Global Change Honest. Global Biogeochemical Cycles, 5, 3, 191-192.

Broecker, W.S., Where has all the carbon gone? 1992: Natural History (in press).

Broecker, W.S., 1992: Upset for Milankovitch theory. Nature, 359, 779-780.

Broecker, W.S., 1992: The Strength of the Nordic heat pump, 13,500 to 9500 B.P., in The Last Deglaciation: Absolute and Radiocarbon Chronologies, ed. E. Bard and W.S. Broecker, p. 173.

Broecker, W.S., 1992: Defining the Boundaries of the Last-Glacial Isotope Episodes (Letter to the Editor). Quarternary Research, 38, 135-138.

Broecker, W.S. and E. Bard, 1992: The Last Deglaciation: Absolute and Radiocarbon Chronologies, NATO ASI Series (Series 1: Global Environmental Change, Vol. 2).

Broecker, W.S., G. Bonani, C. Chen, E. Clark, S. Ivy, M. Klas, and T.-H. Peng, 1992: Evidence for an Early Holocene $CaCO_3$ Preservation Event. Paleoceanography (in press).

Broecker, W.S., G. Bond, M. Klas, E. Clark and J. McManus, 1992: Origin of the Northern Atlantic's Heinrich Events. Climate Dynamics, 6, 265-273.

Broecker, W.S., M. Klas, E. Clark, G. Bonani, S. Ivy and W. Wolfli, 1992: The influence of $CaCO_3$ dissolution on radiocarbon ages for deep-sea sediments, Paleoceanography, 6, 503-608.

Broecker, W.S. and E. Maier-Reimer, 1992: The influence of air and sea exchange on the carbon isotope distribution in the sea. Biogeochemical Cycles (in press).

Broecker, W.S. and T.-H. Peng, 1992a: Interhemispheric transport of CO_2 by ocean circulation. Nature, 356, 587-589.

Broecker, W.S. and T.-H. Peng, 1992b: Dynamic constraints on CO_2 uptake by an iron-fertilized Antarctic, Modeling the Earth System. In: OIES Global Change Institute, Dennis Ojima, ed. 77-105.

Broecker, W.S. and T.-H. Peng, 1992c: What caused the glacial to interglacial CO_2 change? NATO II Ciocco volume (in press).

Broecker, W.S. and T.-H. Peng, 1992d: Interhemispheric transport of $\sum CO_2$ through the ocean. NATO II Ciocco volume (in press).

Broecker, W.S. and T.-H. Peng, 1992e: Does the ^{13}C budget provide a useful constraint on the uptake of fossil fuel CO_2 by the ocean? Global Biogeochemical Cycles (in press).

Broecker, W.S. and J. Severinghaus, 1992: Diminishing Oxygen, Nature, 358, 710-711.

Broecker, W.S. and T. Stocker, 1992: NADW Formation as a Branch of the Hydrological cycle. EOS Transactions, AGU, 73, (18), 202-203.

Broecker, W.S. and F. Woodruff, 1992: Discrepancies in the oceanic carbon isotope record for the last fifteen million years? Garrels Memorial Collection, Geochimica et Cosmochimica Acta, 56, 3259-3264.

Harrison, K., W.S. Broecker and G. Bonani, 1992: A strategy for estimating the impact of CO_2 fertilization on soil carbon storage, Global Biogeochemical Cycles (in press).

Lao, Y., R.F. Anderson, W.S. Broecker, S.E. Trumbore, H.J. Hofmann, W. Wolfli, Increased Production of Cosmogenic ^{10}Be During the Last Glacial Maximum, Nature, 1992a: 357, 576-578.

Lao, Y., R.F. Anderson, W.S. Broecker, S.E. Trumbore, H.J. Hofmann, and W. Wolfli, 1992b: Transport and Burial Rates of ^{10}Be and ^{231}Pa in the Pacific Ocean during the Holocene Period. Earth and Planetary Science Letters, (in press).

Maier,-Reimer, E. and W.S. Broecker, 1992: The Distribution of NADW in the deep ocean: Comparison of Hamburg model with real ocean. Journal of Geophys. Research (in press).

Peng, T.-H., and W.S. Broecker, 1991: Factors limiting atmospheric CO_2 reduction by iron fertilization. Limnology and Oceanography, 36 (8).

Peng, T.-H. and W.S. Broecker, 1992: The Distribution of ^{32}Si in the World Ocean: Model compared to Observation. Global Biogeochemical Cycles (in press).

Peng, T.-H., W.S. Broecker and H.G. Ostlund, 1992: Dynamic Constraints on CO_2 Uptake by an Iron-Fertilized Antarctic. In: Modeling the Earth System, Papers arising from the 1990 OIES Global Change Institute, Dennis Ojima, ed. p. 77-105, UCAR.

Stute, M., P. Schlosser, J.F. Clark, and W.S. Broecker, 1992: Paleotemperatures in the Southwestern

United States derived from noble gases in groundwater. Science, 256, 1000-1002.

White, J.W.C., J. Lawrence, and W.S. Broecker, 1992: Modeling and Interpreting D/H Ratios in Tree Rings: A Test Case of White Pine in the Northeastern United States (in prep.).

Zaucker, F. and W.S. Broecker, 1992: The influence of atmospheric moisture transport on the fresh water balance of the Atlantic drainage basin: GCM simulations and observations, Jour Geophys. Res. 97, 2765-2774.

References

Andrews, J. T. & Tedesco, K., *Geology* (in review).

Broecker, W. S., Bond, G. Klas, M., Clark, E., & McManus, J. *Climate Dynamics* **6**, 265-273 (1992).

Dansgarrd, W., Calusen, H., Gundestrup. N., Hammer, C., Johnsen S., Kristinsdottir, P. & Reeh, N., *Science* **218**, 1273-1277 (1982).

Jantschick, R. & Huon, S., *Ecolg. Geol. Helv.* **85**, (p??) (1992).

Grousset, F. and Chesselet, R. *Earth and Planetary Sci. Lett.* **78**, 271-287 (1986)

Heinrich, H. *Quaternary Research* **29**, 142-152 (1988).

McIntyre,, A., Ruddiman, W.F., & Jantzen, R., *Deep-Sea Research* **19**, 61-77 (1977).

Ruddiman, W., *Geol. Soc. Am. Bull.* **88**, 1813-1827 (1977).

Tedesco, K. & Andrews, J.T. *EOS* **72(44)**, 271 (1992).

Figure Captions

Figure 1. Location of cores containing layers with a high percentage carbonate IRD (ice rafted detritus) and the thicknesses of the first two of those layers (H1 and H2, Fig. 2). The solid black pattern is the distribution of limestone and dolomite bedrock (including submerged rocks in Hudson Bay and Hudson Strait) and the thick solid line is the approximate maximum limit of ice sheets during the last glaciation (refs??). C's are small exposures of carbonate rocks. The Dreizack Area contains cores Me 68-09 and M 01 32 discussed in the text and in Figure 2. The westward increase in thicknesses of layers with carbonate IRD, the Proterozoic K/Ar ages of their fine fraction (Fig. 2) and the widespread occurrence of suitable source rocks in eastern Canada and northwestern Greenland are evidence that the carbonate-bearing icebergs originated in the Labrador Sea-Scotian Shelf regions. Their transit completely across the Atlantic was made possible by extreme cooling of surface waters, as indicated by the high percentages of the ploar planktonic foraminifera *N. pachyderma* in the Heinrich deposits (Fig. 2).

Figure 2. Summary of radiometric, planktonic $\delta^{18}O$, foraminiferal and lithic measurements in cores from DSDP site 609 and from the Dreizack seamount area. The number of forams per gram and the ratio of lithic grains to total entities in cores from both localities defines the six deposits originally identified by Heinrich (1988). Four of these deposits (H1, 2, 4 and 5) contain layers with unusually high percentages of carbonate IRD (ice rafted detritus) determined by line counting the > 150μ fraction with a petrographic microscope. The black bars in DSDP 609 are the positions of these layers in the core as defined by their distinctive appearance in X-radiographs. K/Ar ages of the fine clay fraction in the Dreizack area are evidence of much older source rocks for sediment in layers with carbonate IRD than the ambient sediment. All six Heinrich deposits have high percentages of the polar planktonic foraminifera *N. pachyderma* (l.c.), suggesting that each event occurred at a time of extreme southward penetration of polar surface water. Sharp drops in $\delta^{18}O$ of ~ 1‰ during formation of the first three events suggests that surface salinities were lowered during each event as well. (The gaps in the ratio of *N. pachyderma* to Σ of forams in DSDP site 609 are places where the number of foraminifera is nearly zero.)

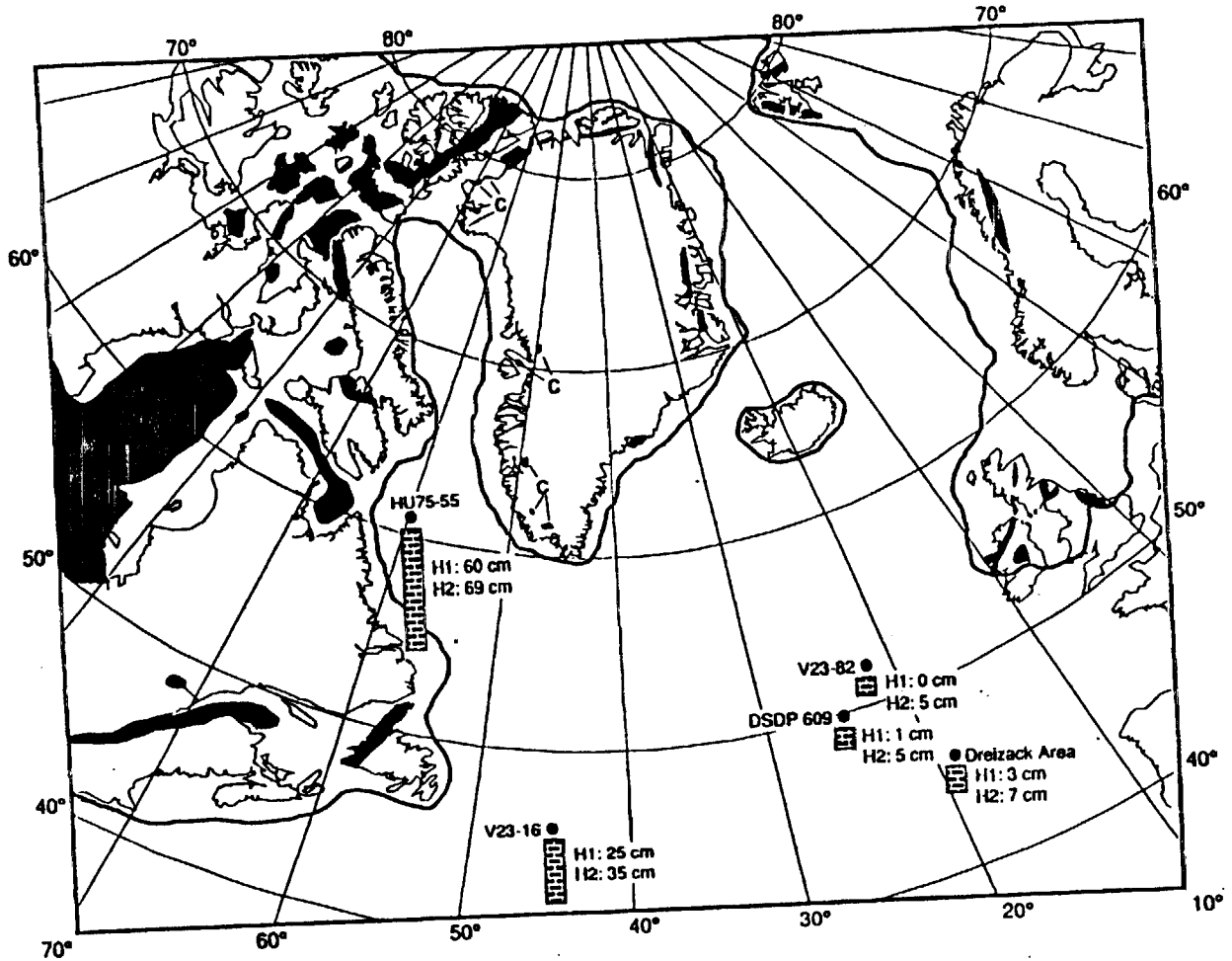
70°
80°
80°
70°
60°
60°
50°
50°
40°
40°
70°
60°
50°
40°
30°
20°
10°
C
C
C
HU75-55
H1: 60 cm
H2: 69 cm
V23-82
H1: 0 cm
H2: 5 cm
DSDP 609
H1: 1 cm
H2: 5 cm
Dreizack Area
H1: 3 cm
H2: 7 cm
V23-16
H1: 25 cm
H2: 35 cm

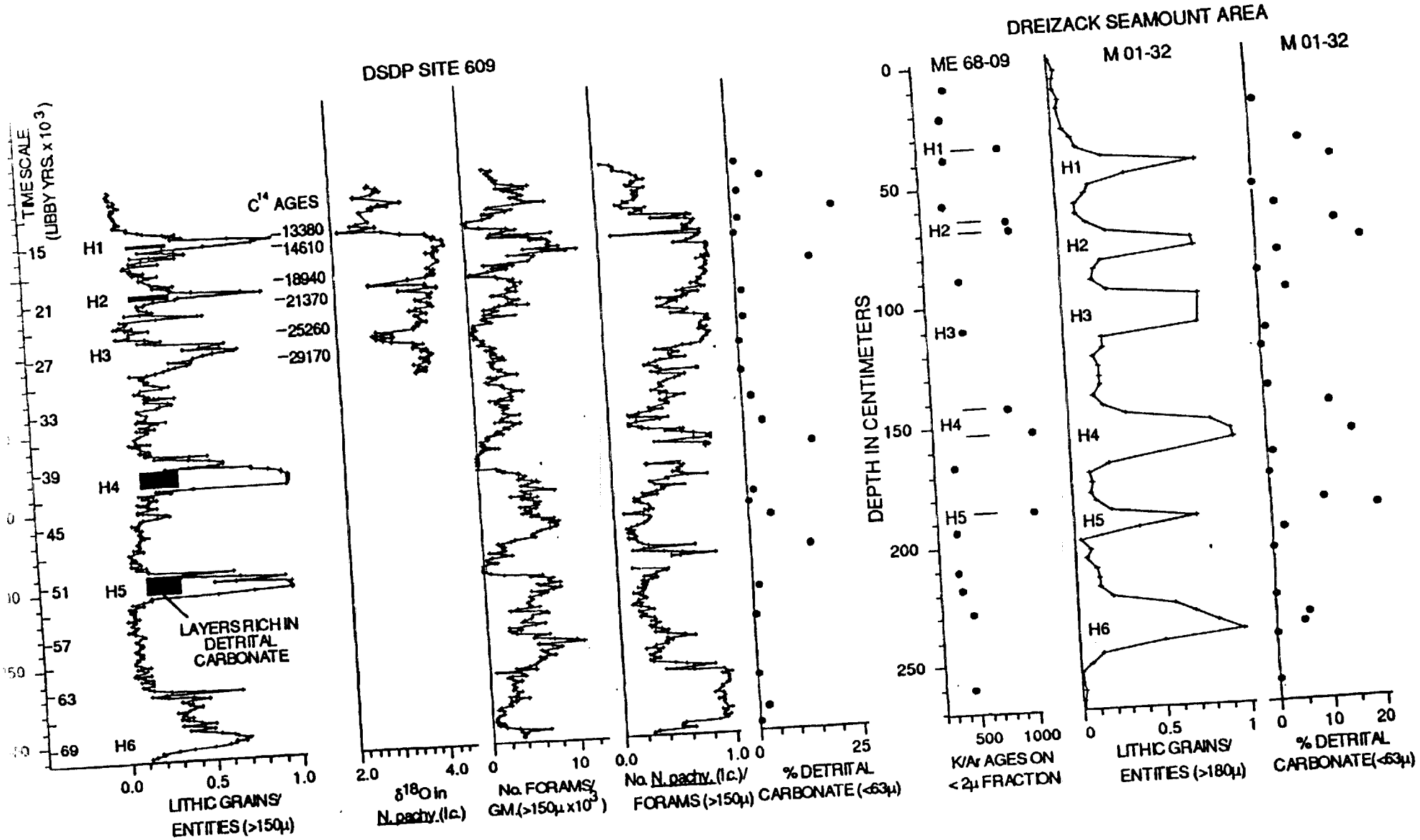
DSDP SITE 609
DREIZACK SEAMOUNT AREA
TIMESCALE (UBBY YRS. x 10⁻³)
C¹⁴ AGES
-13380
-14610
-18940
-21370
-25260
-29170
H1
H2
H3
H4
H5
H6
LAYERS RICH IN DETRITAL CARBONATE
LITHIC GRAINS/ ENTITIES (>150μ)
δ¹⁸O in N. pachy.(l.c.)
No. FORAMS/ GM.(>150μ x10⁻³)
No. N. pachy. (l.c.)/ FORAMS (>150μ)
% DETRITAL CARBONATE (<63μ)
DEPTH IN CENTIMETERS
ME 68-09
M 01-32
M 01-32
K/Ar AGES ON <2μ FRACTION
LITHIC GRAINS/ ENTITIES (>180μ)
% DETRITAL CARBONATE(<63μ)

TABLE 1 Radiocarbon Ages for DSDP 609, V23-16 and HU75-55

Core		Depth (cm)	Corrected Age (years)	Error (years)
DSDP 609		63-65	11880	120
DSDP 609		64-66	11190	200
DSDP 609		69-70	11110	200
DSDP 609		73-75	12440	230
DSDP 609		75-77	13380	230
DSDP 609	H1	84-85	14610	250
DSDP 609		87-88	15910	270
DSDP 609		90-91	16360	150
DSDP 609		105-107	18940	220
DSDP 609		110-111	19900	380
DSDP 609	H2	112-113	21110	220
DSDP 609		115-116	21370	220
DSDP 609		118-120	22380	340
DSDP 609		139-141	25260	440
DSDP 609	H3	143-144	26450	570
DSDP 609		153-155	29170	660
DSDP 609		166-167	29920	800
DSDP 609		174-176	30720	730
V23-16		63	17070	140
V23-16	H2	145	23800	195
V23-16		185	28640	300
V23-16		208	31630	440
HU75-55		81	13185	190
HU75-55	H1	116	14560	105
HU75-55		181	19405	210
HU75-55	H2	250	21508	240

TABLE 2 Foraminifera and IRD sand flux estimates for DSDP 609

	Depth interval (cm)	Radiocarbon time interval	Foraminifera flux (#/cm2 yr)	IRD sand flux (#/cm2 yr)
	64-74	1250	29.78	3.84
	74-76	940	6.54	3.13
H1	76-84	1230	6.62	9.39
	84-87	1300	6.68	3.31
	87-90	450	24.51	10.21
	90-105	2580	26.87	6.07
	105-110	960	10.61	5.13
	110-112	1210	4.19	2.69
H2	112-115	260	8.53	Layer With Carbonate IRD — 20.15
	115-118	1010	9.78	5.25
	118-139	2880	17.24	4.17
	139-143	1190	6.14	1.16
H3	143-153	2720	1.88	2.04
	153-166	750	21.58	11.04
	166-174	800	18.21	5.62

Flux estimates were calculated using measured dry sample weights, sand grain and foram counts, radiocarbon age intervals, and dry bulk density. Dry bulk density was calculated using data from the Ocean Drilling Project, including wet bulk density and sediment porosity. Two equations were solved: Flux = I Σ (#/gm) DBD / Δt , and DBD = WBD - (P psea) , where I = sampling interval, # = particle count, DBD = dry bulk density, Δt = time interval based on radiocarbon, WBD =wet bulk density, P = sediment porosity, and psea = density of seawater.